2 mic

UILU-ENG-74-2001

CIVIL ENGINEERING STUDIES

PHOTOGRAMMETRY SERIES NO. 37

CR-134195

TREATMENT OF CONTROL DATA IN LUNAR PHOTOTRIANGULATION

(Final Technical Report)

By

K. W. WONG

A report on a study

sponsored by

NASA-LYNDON B. JOHNSON SPACE CENTER

Contract No. NAS9-12446

UNIVERSITY OF ILLINOIS AT URBANA-CHAMPAIGN

URBANA, ILLINOIS

JANUARY 1974

TREATMENT OF
CONTROL DATA IN LUNAR PHOTOTRIANGULATION

Final Technical Report
by
Dr. Kam W. Wong
Principal Investigator

January 1974

for

NASA-Lyndon B. Johnson Space Center
Houston, Texas 77058
Contract No. NAS9-12446

Prepared by

Department of Civil Engineering
University of Illinois at Urbana-Champaign
Urbana, Illinois 61801

TABLE OF CONTENTS

1. INTRODUCTION

The positional accuracy of photo-triangulated ground points can be evaluated either by the use of accurate check points or by statistical analysis based on the principles of error propagation. In conventional engineering applications of aerotriangulation, some known ground points are usually withheld from the aerotriangulation solution and are used to serve as ultimate check on the accuracy of the aerotriangulation process. Complete reliance on statistical analysis procedure is not an advisable or common practice.

However, in lunar phototriangulation, there is a complete lack of accurate ground control points. The accuracy analysis of the results of lunar phototriangulation must, therefore, be completely dependent on statistical procedure. It was the objective of this investigation to examine the validity of the commonly used statistical procedures, and to develop both mathematical techniques and computer softwares for evaluating 1) the accuracy of lunar phototriangulation; 2) the contribution of the different types of photo support data on the accuracy of lunar phototriangulation; 3) accuracy of absolute orientation as a function of the accuracy and distribution of both the ground and model points; and 4) the relative slope accuracy between any triangulated pass points.

These statistical techniques were applied to evaluating the triangulation and mapping accuracy of the mapping system flown in the Apollo 15, 16 and 17 missions. The system included a 76-mm. metric camera with a 74°x74° field of view and a frame size of 114x114 mm. The camera had a glass reseau plate containing 121 reseau crosses at the focal plane. The camera provided 1:1,450,000 photography at a nominal altitude of 110 km. with a ground resolution of 20 m. A 76-mm. stellar camera took pictures of the star field to provide attitude controls for the mapping camera. The two cameras were timed for simultaneous exposures. Scale control was provided by a laser altimeter which had a designed range accuracy of ± 2 m. Also included in the system was a 610-mm. optical bar panoramic camera. It had a 10°46'x108° field with an image size of 114x1,148 mm. At an altitude of

110 km, its photography had a scale of approximately 1:180,000 at the center of the frame with a resolution of about 1 to 2 m. The panoramic camera was tilted alternately forward and backward 12.5° so that consecutive frames of similar tilt had 10% overlap and stereopairs had 100% overlap. It provided sterocoverage of a strip approximately 330 km. wide, centered on the ground tracks.(5)

The 76-mm. mapping camera photography is being used by NASA to establish a network of lunar controls by means of phototriangulation. The high-resolution panoramic photography is used to produce large scale lunar maps. The pass points obtained from the triangulation of the 76-mm. photography will be used as ground controls in the absolute orientation of the stereomodels from the panoramic photography. In this investigation, the relative accuracy of the triangulated pass points was evaluated by a simulation process; and the accuracy of the absolute orientation process was evaluated using real data provided by NASA.

Mr. Nick G. Yacoumelos was the research assistant in this project when he was studying for the doctorate degree at the University of Illinois at Urbana-Champaign. He did an extensive literature research on the method of propagation of variance, and assisted ably in both data processing and data analysis. He is presently an Assistant Professor at the Lowell Institute of Technology.

Mr. Robert Hill of the Mapping Sciences Branch at the Lyndon B. Johnson Space Center was the technical contract monitor for NASA. AS-11-B1 data on one model of 76-mm. photography and three models of panoramic photography from the Apollo 15 mission was provided by the Lockheed Electronics Company in cooperation with Mr. Robert Hill.

2. THEORETICAL BASIS OF THE METHOD OF PROPAGATION OF VARIANCE

In the application of the least-squares method in analytical photogrammetry, the variance-covariance matrix of the unknown parameters is commonly computed as the inverse of the normal equation multiplied by the standard error of unit weight. For example, in the simultaneous solution for phototriangulation, the solution equations may be summarized as follows(4):

$$\delta = N^{-1}C; \tag{2.1}$$

and

$$\delta_j = N_j^{-1}C_j - Q_j\delta \quad \text{for all pass points } j; \tag{2.2}$$

where δ is a matrix of the unknown corrections to all the exterior orientation parameters (i.e. $\Delta\omega_i$, $\Delta\phi_i$, $\Delta\kappa_i$, ΔX_i^C, ΔY_i^C and ΔZ_i^C); and δ_j is a matrix of the unknown corrections to the coordinates of point j, i.e. ΔX_j, ΔY_j and ΔZ_j. The following expressions for the variance-covariance matrices were originally developed by Brown and have been used in common practice(2), (4):

$$\sigma_\delta = \sigma_o^2 N^{-1}, \tag{2.3}$$

and

$$\sigma_{\delta j} = \sigma_o^2 N_j^{-1} + Q_j\sigma_\delta Q_j^T. \tag{2.4}$$

This method of the propagation of variance was a direct extension of the technique which was developed for direct linear least-squares regression, which has been treated extensively in textbooks on statistics (1), (7). Although many authors (8, 9) have discussed the problems of iterative least-squares adjustment in geodetic and photogrammetric literature, there has been no critical examination into the validity of Brown's formulation.

This investigation showed that Brown's formulation is theoretically valid in direct least-squares solution, in which the original observation equations are linear functions of the unknowns. In iterative least-squares solution, as required by most photogrammetric problems, this

formulation is valid only if the unknown corrections (δ and δ_j in equation (2.1) and (2.2) respectively) converge to zero. In Section 2.1, the theoretical basis of this formulation for a direct least-squares solution is examined; and in Section 2.2, the condition under which the formulation becomes invalid for an iterative solution will be discussed.

2.1 Direct Linear Least-Squares Solutions

2.1.1 A Linear Regression Model

Consider a simple problem in linear regression. Figure 1 presents the result of an experiment in which the value of a variable y was measured at various values of x. Let it be assumed that, in the absence of any error in the measurements, the variable y should be a linear function of x; i.e.

$$y = a_o + a_1 x \tag{2.5}$$

Furthermore, let it be assumed that the measurement of the variable x can be made exactly. Thus, the only explanation for not having all the points in Fig. 1 lying in a straight line is the presence of random errors in the measurement of the variable y. Thus, for point i in Fig. 1, the following error equation can be generated:

$$y_i - v_i = a_o + a_1 x_i$$

where v_i is the random error in the measured value y_i. Rearranging terms, the above equation may be expressed as follows:

$$v_i + a_o + a_1 x_i = y_i \tag{2.6}$$

In matrix notation,

$$[v_i] + [1 \; x_i] \begin{bmatrix} a_o \\ a_1 \end{bmatrix} = [y_i]$$

i.e. $$V_i + B_i A = Y_i \tag{2.7}$$

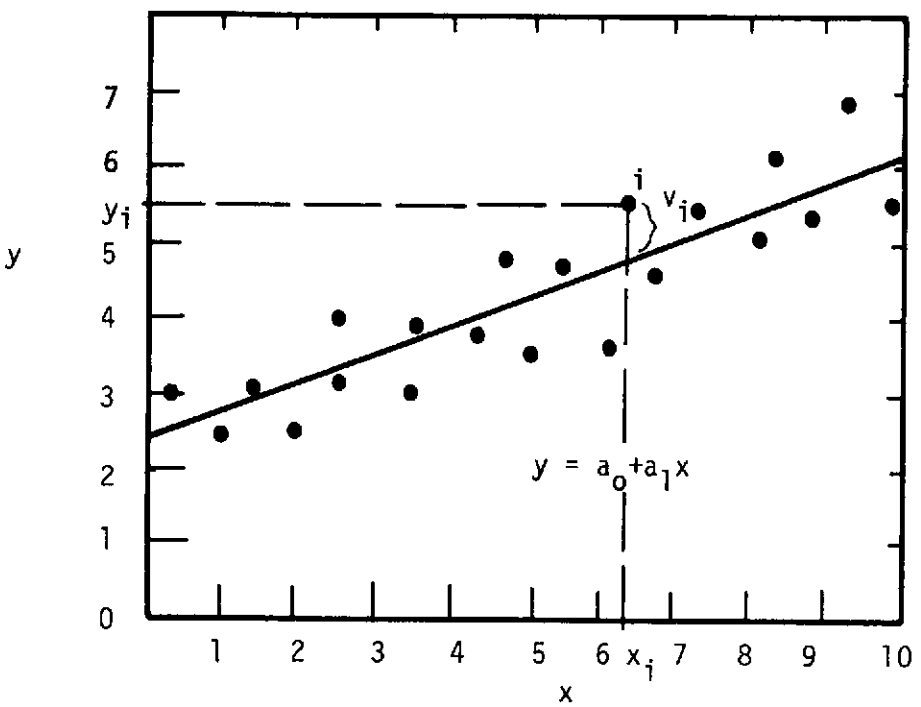

Fig. 1. A Linear Regression Problem

With one equation generated by each measurement of y, m points will generate m equations which may be combined together as follows:

$$\begin{bmatrix} V_1 \\ V_2 \\ \cdot \\ \cdot \\ \cdot \\ V_m \end{bmatrix} + \begin{bmatrix} B_1 \\ B_2 \\ \cdot \\ \cdot \\ \cdot \\ B_m \end{bmatrix} A = \begin{bmatrix} Y_1 \\ Y_2 \\ \cdot \\ \cdot \\ \cdot \\ Y_m \end{bmatrix}$$

i. e. $$V + B \cdot A = Y \tag{2.8}$$

It can be easily derived that the corresponding normal equations will be

$$(B^T W B) \cdot A = B^T W Y \tag{2.9}$$

where W is the weight matrix for the measured values of y and is defined as follows:

$$W = \sigma_o^2 \sigma_Y^{-1} \tag{2.10}$$

where σ_o is the standard error of unit weight; σ_Y is the covariance-covariance matrix of the measured values of y.

Let $$N = B^T W B, \text{ and } C = B^T W Y \tag{2.11}$$

The most probable value of the coefficients a_o and a_1 can then be computed as

$$A = N^{-1} C. \tag{2.12}$$

It can be theoretically proved that, for this solution under the given set of assumptions, the variance-covariance matrix for the computed coefficients may be simply expressed as

$$\sigma_A = \sigma_o^2 N^{-1}. \tag{2.13}$$

2.1.2 Statistical Definition of Variance and Covariance

Before attempting to derive Eq. (2.13), the statistical definitions of mathematical expectation, variance and covariance are first reviewed (7). Let X be a random variable which can take on the values of $x_1, x_2, x_3, \ldots x_n$ with the probability $p_1, p_2, p_3, \ldots p_n$ respectively. Then, the expected value of X, denoted as E(X), is defined as

$$E(X) = \sum_{i=1}^{n} x_i p_i \tag{2.14}$$

The expected value of X is also called the population mean of X. If X is a continuous random variable which has a probability distribution function f(x), then the expected value is defined as

$$E(X) = \int_{-\infty}^{\infty} xf(x)dx \tag{2.15}$$

It can be easily proved that if b is a constant scaler, then E(bX) = bE(X).

The variance of the variable X is defined as follows:

$$\sigma_X = E\{(X-E(X))^2\} . \tag{2.16}$$

The covariance σ_{XY} between two random variables X and Y is defined as follows:

$$\sigma_{XY} = \{E\ (X-E(X))\ (Y-E(Y))\} \tag{2.17}$$

Let Z be a column matrix of random variables $Z_1, Z_2, Z_3, \ldots Z_m$, i.e.

$$\underset{(m,1)}{Z} = \begin{bmatrix} Z_1 \\ Z_2 \\ \cdot \\ \cdot \\ \cdot \\ Z_m \end{bmatrix}$$

Then, it can be easily derived from the above fundamental definition that the variance-covariance matrix for Z may be expressed as follows:

$$\sigma_Z = E\{(Z-E(Z))\ (Z-E(Z))^T\} \tag{2.18}$$

where σ_Z is an (mxm) matrix.

2.1.3 Derivation of the Variance-Covariance Matrix

The variance-covariance matrix of the unknown matrix A in Eq. (2.12) can thus be expressed as follows:

$$\sigma_A = E\{(A-E(A))\ (A-E(A))^T\} \tag{2.19}$$

Substituting Eq. (2.11) and (2.10) into the above expression yields

$$\sigma_A = E\{(N^{-1}C - E(N^{-1}C))(N^{-1}C-E(N^{-1}C))^T\} \tag{2.20}$$

But $E(N^{-1}C) = E(N^{-1}B^TWY)$. Since Y is the only matrix consisting of variable parameters,

$$E(N^{-1}C) = E(N^{-1}B^TWY) = N^{-1}B^TWE(Y)$$

Therefore, Eq. (2.20) may be expressed as

$$\begin{aligned}\sigma_A &= E\{(N^{-1}B^TWY - N^{-1}B^TWE(Y))(N^{-1}B^TWY-N^{-1}B^TWE(Y))^T\} \\ &= E\{(N^{-1}B^TW(Y-E(Y))(Y-E(Y))^TWBN^{-1}\} \\ &= N^{-1}B^TWE\{(Y-E(Y))(Y-E(Y))^T\}WBN^{-1}\end{aligned}$$

By definition,

$$\sigma_Y = E\{(Y-E(Y))(Y-E(Y))^T\}$$

From Eq. (2.10), $\sigma_Y = \sigma_o^2W^{-1}$,

Therefore,

$$\sigma_A = \sigma_o^2 N^{-1} B^T W W^{-1} W B N^{-1}$$

$$= \sigma_o^2 N^{-1} (B^T W B) N^{-1}$$

$$= \sigma_o^2 N^{-1} N N^{-1}$$

Hence $\sigma_A = \sigma_o^2 N^{-1}$;

which is Eq. (2.13).

In summary, it can be stated that in a given least-squares adjustment problem, if the observation model may be expressed as

$$V + B \cdot A = Y;$$

and if the only random variables included in the matrix Y are the measured parameters; then the variance-covariance matrix of the unknown matrix may be computed as

$$\sigma_A = \sigma_o^2 N^{-1}.$$

It will be shown in the Section 2.3 that the second condition is not necessarily satisfied in an iterative least-squares solution.

2.2 Iterative Least-Squares Solutions

2.2.1 Simultaneous Solution for Aerotriangulation

When the observation equations are non-linear functions, an iterative least-squares solution is generally required. As an example, consider the solution model for the simultaneous adjustment of photogrammetric blocks. The mathematical formulation for this solution method has been well documented in the literature and will therefore only be presented here in summarized form.

The solution is based on the following pair of collinearity equations which relate the image coordinates (x_{ij}, y_{ij}) to the ground coordinates (X_j, Y_j and Z_j):

$$F_x = x_{ij} - x_p + \frac{f[m_{11}(X_j - X_i^c) + m_{21}(Y_j - Y_i^c) + m_{31}(Z_j - Z_i^c)]}{[m_{13}(X_j - X_i^c) + m_{23}(Y_j - Y_i^c) + m_{33}(Z_j - Z_i^c)]} = 0$$

and

$$F_y = y_{ij} - y_p + \frac{f[m_{12}(X_j - X_i^c) + m_{22}(Y_j - Y_i^c) + m_{32}(Z_j - Z_i^c)]}{[m_{13}(X_j - X_i^c) + m_{23}(Y_j - Y_i^c) + m_{33}(Z_j - Z_i^c)]} = 0 \qquad (2.21)$$

where x_p and y_p are the image coordinates of the principal point; f is the focal length; X_i^c, Y_i^c and Z_i^c are ground coordinates of the ith camera position during the exposure; and the m_{ij}'s are functions of the three rotation parameters (ω_i, ϕ_i, κ_i) of the camera.

By first-order Newton approximation, the collinearity equations may be linearized as follows:

$$V_{x_{ij}} + \left(\frac{\partial F_x}{\partial X_i^c}\right)^o \Delta X_i^c + \left(\frac{\partial F_x}{\partial Y_i^c}\right)^o \Delta Y_i^c + \left(\frac{\partial F_x}{\partial Z_i^c}\right)^o \Delta Z_i^c + \left(\frac{\partial F_x}{\partial \omega_i}\right)^o \Delta\omega_i + \left(\frac{\partial F_x}{\partial \phi_i}\right)^o \Delta\phi_i$$

$$+ \left(\frac{\partial F_x}{\partial \kappa_i}\right)^o \Delta\kappa_i + \left(\frac{\partial F_x}{\partial X_j}\right)^o \Delta X_j + \left(\frac{\partial F_x}{\partial Y_j}\right)^o \Delta Y_j + \left(\frac{\partial F_x}{\partial Z_j}\right)^o \Delta Z_j = \varepsilon_{x_{ij}}$$

$$V_{y_{ij}} + \left(\frac{\partial F_y}{\partial X_i^c}\right)^o \Delta X_i^c + \left(\frac{\partial F_y}{\partial Y_i^c}\right)^o \Delta Y_i^c + \left(\frac{\partial F_y}{\partial Z_i^c}\right)^o \Delta Z_i^c + \left(\frac{\partial F_y}{\partial \omega_i}\right)^o \Delta\omega_i + \left(\frac{\partial F_y}{\partial \phi_i}\right)^o \Delta\phi_i$$

$$+ \left(\frac{\partial F_y}{\partial \kappa_i}\right)^o \Delta\kappa_i + \left(\frac{\partial F_y}{\partial X_j}\right)^o \Delta X_j + \left(\frac{\partial F_y}{\partial Y_j}\right)^o \Delta Y_j + \left(\frac{\partial F_y}{\partial Z_j}\right)^o \Delta Z_j = \varepsilon_{y_{ij}} \qquad (2.22)$$

where

$$\varepsilon_{x_{ij}} = -[x_{ij}-x_p + \frac{f[m_{11}(X_j^o-X_i^{co}) + m_{21}(Y_j^o-Y_i^{co}) + m_{31}(Z_j^o-Z_i^{co})]}{[m_{13}(X_j^o-X_i^{co}) + m_{23}(Y_j^o-Y_i^{co}) + m_{33}(Z_j^o-Z_i^{co})]}$$

and

$$\varepsilon_{y_{ij}} = -[y_{ij}-y_p + \frac{f[m_{12}(X_j^o-X_i^{co}) + m_{22}(Y_i^o-Y_i^{co}) + m_{32}(Z_j^o-Z_i^{co})]}{[m_{13}(X_j^o-X_i^{co}) + m_{23}(Y_j^o-Y_i^{co}) + m_{33}(Z_j^o-Z_i^{co})]}$$

(2.23)

where X_j^o, Y_j^o, Z_j^o are approximate ground coordinates of point j,

X_i^{co}, Y_i^{co}, Z_i^{co} are approximate ground coordinates of the ith camera position

$(\frac{\partial F_x}{\partial X_i^c})^o$, $(\frac{\partial F_y}{\partial X_i^c})^o$, etc. are partial derivatives of Eq. (2.21) computed using the approximate values of all the parameters.

Equation 2.22 may be expressed in matrix notation as

$$\dot{V}_{ij} + \dot{B}_{ij}\dot{\Delta} + \ddot{B}_{ij}\ddot{\Delta}_j = \dot{\varepsilon}_{ij} \qquad (2.24)$$

where $\dot{\Delta}$ is a matrix of the corrections to exterior orientation parameters (ΔX_i^c, ΔY_i^c, ΔZ_i^c, $\Delta\omega_i$, $\Delta\phi_i$, $\Delta\kappa_i$) of all camera stations; and $\ddot{\Delta}_j$ is the matrix of the corrections to the ground coordinates of point j.

The complete set of observation equations for all measured image coordinates will take the following matrix form:

$$\dot{V} + \ddot{B}\Delta + \ddddot{B}\Delta = \dot{\varepsilon};$$

which may also be simply written as

$$\dot{V} + B\Delta = \dot{\varepsilon} \qquad (2.25)$$

An observation equation may also be written for each coordinate of a known control point and for each known exterior orientation elements.

For example, the observation equations for a known control point with measured coordinates $(X_j^{oo}, Y_j^{oo}, Z_j^{oo})$ are as follows:

$$\begin{aligned} \ddot{v}_{X_j} - \Delta X_j &= X_j^o - X_j^{oo} \\ \ddot{v}_{Y_j} - \Delta Y_j &= Y_j^o - Y_j^{oo} \\ \ddot{v}_{Z_j} - \Delta Z_j &= Z_j^o - Z_j^{oo} \end{aligned} \tag{2.26}$$

In matrix notation:

$$\ddot{V}_j - \ddot{\Delta}_j = \ddot{\varepsilon}_j \tag{2.27}$$

In general, the complete set of control data may be represented by the following equation:

$$\ddot{V} - \Delta = \ddot{\varepsilon} \tag{2.28}$$

Therefore, combining Eq. (2.25) and (2.26), the complete mathematical model is as follows:

$$\dot{V} + B\Delta = \dot{\varepsilon}$$

$$\ddot{V} - \Delta = \ddot{\varepsilon}$$

which may be simply expressed as

$$V + B\Delta = \varepsilon, \tag{2.29}$$

The normal equations will be

$$(B^T W B)\Delta = B^T W \varepsilon \tag{2.30}$$

where W is the weight matrix for the observations.

The least-squares solution for Δ is then obtained by the solution of the above normal equations; i.e.

$$\Delta = N^{-1} C \tag{2.31}$$

where $N = (B^T WB)$ and $C = B^T W\varepsilon$.

However, because of the first-order approximation used in the linearization of the collinearity equations, the least-square solution must be iterated until the corrections (Δ) become negligibly small. It will be shown in the next section that the convergence of the Δ-matrix is the necessary condition for the expression $\sigma_\Delta = \sigma_o^2 (B^T WB)^{-1}$ to be valid.

2.2.2 Derivation of the Variance-Covariance Matrix

The normal equation in Eq. (2.30) is in exactly the same form as the normal equation in Eq. (2.9). Therefore, the derivation procedure should be identical to that presented in Section 2.1.3 until the following expression is reached:

$$\sigma_\Delta = N^{-1} B^T WE\{(\varepsilon - E(\varepsilon))(\varepsilon - E(\varepsilon))^T\} WBN^{-1}$$

Since, by definition, $E\{(\varepsilon - E(\varepsilon))(\varepsilon - E(\varepsilon))^T\} = \sigma_\varepsilon$,

$$\sigma_\Delta = N^{-1} B^T W \sigma_\varepsilon WBN^{-1}. \qquad (2.32)$$

Two conditions of convergence of the least-squares solution are next considered separately.

a) Convergence with Δ approaches zero.

As Δ becomes zero, Eq. (2.29) becomes

$$V = \varepsilon.$$

That is, the residual terms $\varepsilon_{x_{ij}}$ and $\varepsilon_{y_{ij}}$ in Eq. (2.23) and the residual terms ε_j in Eq. (2.27) are caused only by errors in the measured parameters. Therefore, the approximation parameters in these observation equations have become constant parameters and the only random variables in the residual terms are the measured parameters. Let σ^{oo} denotes the variance-covariance matrix of all the observations. Then it is obvious that under this condition of convergence, the following relationship is true:

$$\sigma_{\varepsilon} = \sigma^{oo} \tag{2.33}$$

Since by definition, $W = \sigma_o^2 \, (\sigma^{oo})^{-1}$,

$$\sigma_{\varepsilon} = \sigma^{oo} = \sigma_o^2 \, W^{-1} \tag{2.34}$$

By substituting Eq. (2.34) into Eq. (2.32), it can be easily shown that again

$$\sigma_{\Delta} = \sigma_o^2 \, N^{-1} .$$

Let X^o denote the matrix of all the approximate parameters, and X denotes the matrix of all the unknown parameters; i.e.

$$X = X^o + \Delta$$

Then, since X^o has stabilized to become a constant term, the variance-covariance matrix of the computed values of the unknowns is equal to the variance-covariance matrix of the corrections; i.e.

$$\sigma_X = \sigma_{\Delta}$$

b) Solution stabilized but Δ fails to approach zero.

In a weakly conditioned photogrammetric solution, such as that caused by poor geometry or low-accuracy controls, some or all of the correction parameters may never approach zero. After a certain number of iterations, these correction parameters may simply oscillate between certain boundary limits from iteration to iteration. If the iteration procedure is allowed to continue, such a solution will eventually begin to diverge rapidly.

In such a solution, the residual terms in the observation equations will include measurement errors, approximation errors, and errors introduced by the linearization of the observation equations. It is no longer true that the variance-covariance matrix of these residual terms is equal to the variance-covariance matrix of the measurements; i.e.

$$\sigma_{\varepsilon} \neq \sigma^{00}$$

Consequently, $\sigma_{\Delta} \neq \sigma_{o}^{2} N^{-1}$.

There is no statistical method available for directly computing σ_{ε} from the solution.

3. ACCURACY ANALYSIS IN LUNAR PHOTOTRIANGULATION

3.1 Computer Program SAPGO-A

A computer program was developed for performing complete error analysis on lunar phototriangulation. It is based on the principle of propagation of variance, as described in Chapter 2. The program may be used for either the triangulation of real photogrammetric data, or for simulation study using fictitious data. It can accept as input the following types of data:

1) photographic image coordinates with a specified variance-covariance matrix for all points;
2) ground controls with known rectangular ground coordinates (X_j, Y_j and Z_j) and the corresponding variance-covariance matrix for each control point;
3) distances, horizontal angles and azimuths measured on the lunar surface with the corresponding standard error for each measurement;
4) the position of any exposure station in rectangular coordinates (X_i^c, Y_i^c and Z_i^c) with its corresponding variance-covariance matrix;
5) the orientation of the camera axis defined by the three rotation angles ω, ϕ, and κ at each camera station, together with the corresponding variance-covariance matrix;
6) the straight-line distance between a camera station and any ground point, together with its standard error; and
7) the known ground coordinates of a set of check points.

The output of the program includes the following:

1) the correction parameters at the end of each iteration;
2) the computed standard error of unit weight at the end of each iteration;
3) the final adjusted values of the exterior orientation parameters and their estimated standard errors ($X_i^c \pm \sigma_{X_i}^c$, $Y_i^c \pm \sigma_{Y_i}^c$, $Z_i^c \pm \sigma_{Z_i}^c$, $\omega_i \pm \sigma_{\omega_i}$, $\phi_i \pm \sigma_{\phi_i}$, and $\kappa_i \pm \sigma_{\kappa_i}$);

4) the final adjusted ground coordinates of all the pass points and their standard errors; and
5) the true errors at the check points.

This program was a modified version of the SAPGO-A program which was originally designed for aerotriangulation in earth application. SAPGO is the acronym for simultaneous adjustment of photogrammetric and geodetic observations. The mathematical formulation of the solution has been published in (5). The modified version of SAPGO-A is equally applicable for both lunar and earth application, and a full documentation of the program is being prepared (6).

3.2 A Simulation Model

A simulation was conducted to achieve two objectives: 1) to test the reliability of the method of accuracy analysis in the computer program SAPGO-A; and 2) to evaluate the contribution of the various types of control data on the accuracy of lunar phototriangulation.

Fictitious data was generated by a computer program called DTAGEN, which was developed at the University of Illinois. For a given flight configuration specified by the camera focal length, flight altitude, percentage overlap, origin of the reference coordinate system, and position of the first exposure; program DTAGEN generates all the necessary photo image coordinates, exterior orientation parameters, and ground coordinates of all corresponding image points. To simulate the measurement errors in practice, these parameters were perturbed according to some specified standard errors. Both the perturbed and the true values of all of these parameters were provided by the program.

The simulation model in this study consisted of a strip of 11 photos having the same flight configuration as the 76-mm. metric photography from the Apollo 15 mission. The flight attitude was 110 Km and the longitudinal overlap was 60%. There were 25 pass points arranged in a 5x5 rectangular pattern in each photo, and the photo coordinates were perturbed with a standard error of ± 5 μm.

Three types of control data were generated: 1) laser altimeter measurement; 2) attitude data (ω_i, ϕ_i, κ_i) for the camera; and 3) tracking data. The laser altimeter measurements were the straight-line distances between the camera stations and the pass points located at

that center of the photos. These distances were perturbed with a standard error of ± 3 m. The camera attitude data were perturbed with the following standard errors: $\sigma_\omega = \pm 10''$, $\sigma_\phi = \pm 20''$, and $\sigma_\kappa = \pm 10''$. These accuracy levels have been found to be realistic from the analysis of actual data from the Apollo 15 mission (7).

In reality, the tracking data for each orbit consisted of a position vector in the epoch, velocity vector of the orbit, and time of exposure with respect to the epoch. These data can be used to constraint the position of the exposure stations. Since the objective of this study was to determine the internal accuracy of the photogrammetric solution rather than the absolute positioning accuracy, the exterior orientation parameters (X^C, Y^C, Z^C, ω, ϕ, and κ) of the first photo in the strip was held fixed and assumed to be error free.

Helmering (7) reported that, from the analysis of three strips of Apollo 15 photography, the attainable accuracy for the velocity vector was about ± 0.1 meter per second while the timing accuracy was ± 1 millisecond. In this study, simulation runs were performed using three different levels of accuracy in the velocity vector: ± 0.1, ± 0.5 and ± 1.0 meter per second. The relative timing accuracy was assumed to be ± 1 millisecond. At these accuracy levels, the corresponding uncertainty in the coordinates of the exposure stations corresponds to those listed in Table 1. All three coordinates (X_j^C, Y_j^C, Z_j^C) of each exposure station were assumed to have the same standard error.

3.3 Experimental Verification on the Propagation of the Variance

3.3.1 Well-controlled photography

Figures 2, 3, 4 and 5 show the results of a series of simulation using various combination of control data. A tracking accuracy of ± 0.5 m/sec. for the velocity vector was assumed for all cases; i.e. the exposure station coordinates were weighted according to the standard errors listed in column 2 of Table 1. The following four combinations of controls were used:

Table 1. Standard Errors of Exposure Station Coordinates for Three Levels of Velocity Vector Accuracy (σ_V) ($\sigma_{X_i^c} = \sigma_{Y_i^c} = \sigma_{Z_i^c}$)

Photograph	Std. Errors of Exposure Station Coordinates		
	$\sigma_V = \pm 0.1$ m/sec.	$\sigma_V = \pm 0.5$ m./sec.	$\sigma_V = \pm 1.0$ m./sec.
1	0	0	0
2	± 4 m.	± 20 m.	± 40 m.
3	6	29	57
4	7	35	70
5	8	40	81
6	9	45	90
7	10	50	99
8	11	54	107
9	12	57	114
10	12	61	121
11	13	64	128

1) tracking data alone (Fig. 2);
2) tracking data and altimeter measurements (Fig. 3);
3) tracking data and attitude measurements (Fig. 4); and
4) tracking, altimeter and attitude data (Fig. 5).

Five independent strips of 11 photos were triangulated. In these figures, the true errors in the adjusted coordinates of the pass points located near the center of each photo are plotted against the estimated RMS error computed from the propagation of variance. With the exception of a few data points, all the true errors felt within the three sigma value of the computed RMS errors. Thus, the RMS errors present a realistic evaluation of the accuracy of the computed coordinates.

Tables 2, 3 and 4 list the estimated RMS errors versus the true errors in the computed coordinates of the exposure stations for five cases in which tracking, altimeter and attitude data were all used as controls. Also listed in these tables are the magnitude of the correction parameters in the last iteration of the iterative least-squares solution. Except in case 5 of Table 4, all the corrections were less than the estimated RMS errors of the parameters.

3.3.2 Poorly Controlled Photography - Cantilever Extension

Figures 6, 7 and 8 show the true errors in the computed coordinates of the center pass points for a cantilever strip. The exterior orientation parameters of both the first and second photo in the strip were held fixed in the solution. The strip was not controlled by any other control data. Five independent strips were triangulated, and the true errors were plotted in these figures against the three-sigma value of the estimated RMS errors.

These figures show rapid accumulation of systematic errors in the phototriangulation process. Furthermore, the systematic pattern varies from strip to strip. The computed RMS errors failed to detect these systematic errors and clearly underestimated the inaccuracy of the solution.

Tables 5, 6 and 7 list the true errors in the computed coordinates of the exposure stations for the same cases. The magnitude of the corrections in the last iteration are also listed. It was observed that beyond station No. 7, the corrections generally exceeded the estimated RMS error of these parameters.

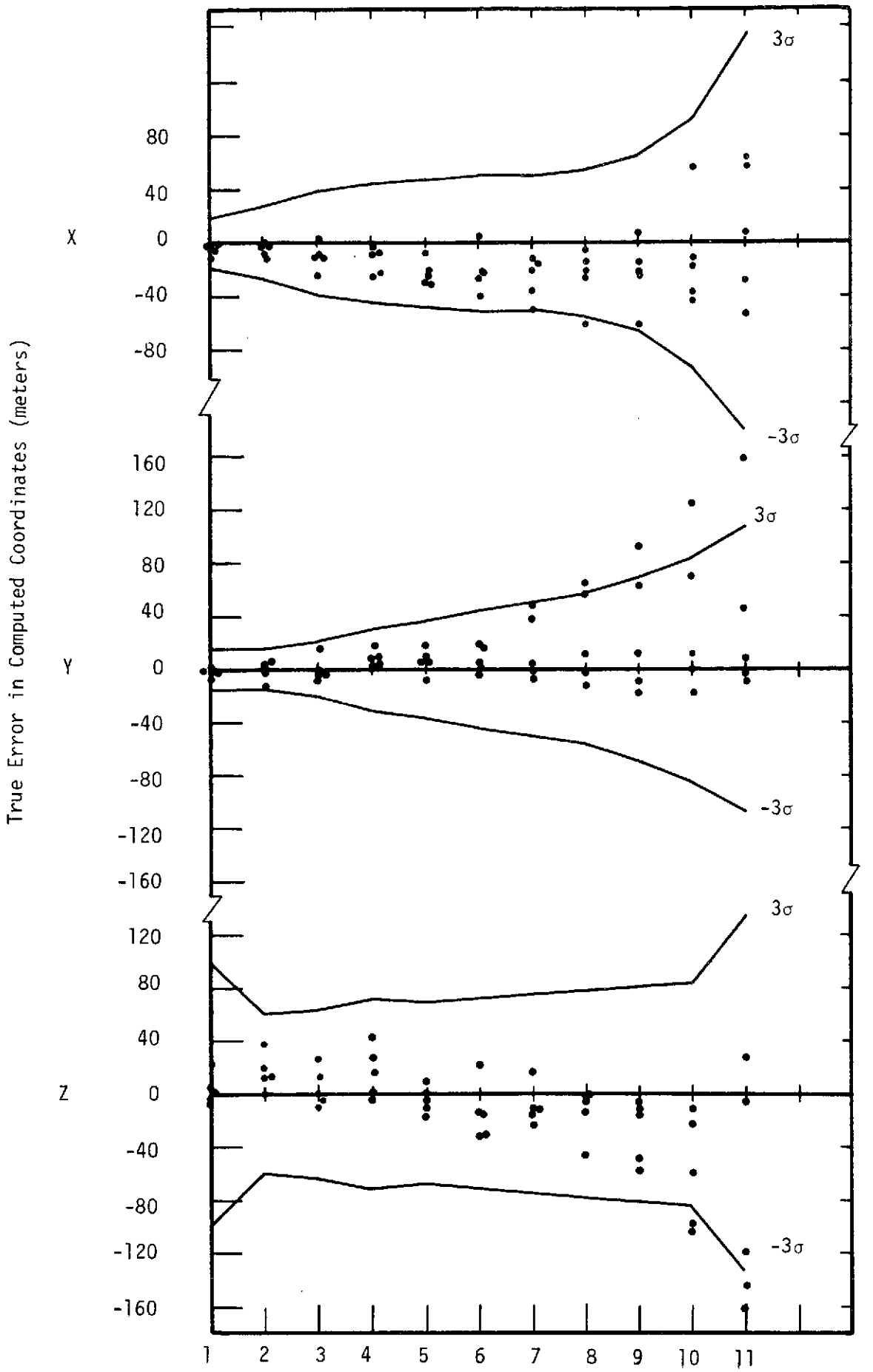

Fig. 2. True Error in Computed Pass Point Coordinates of Five Cases (Tracking Controls Only)

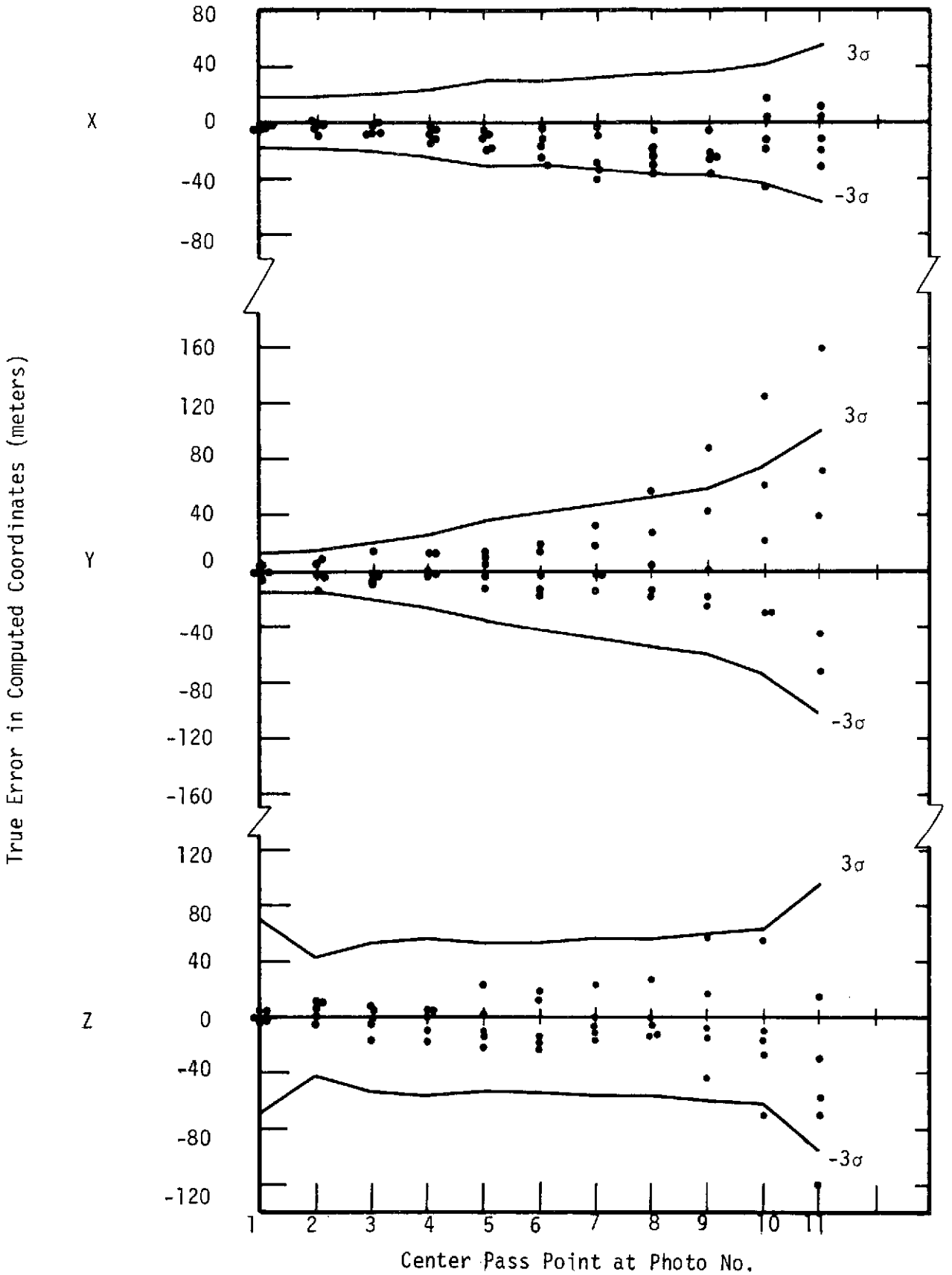

Fig. 3. True Error in Computed Pass Point Coordinates of Five Cases (Tracking + Altimeter Controls)

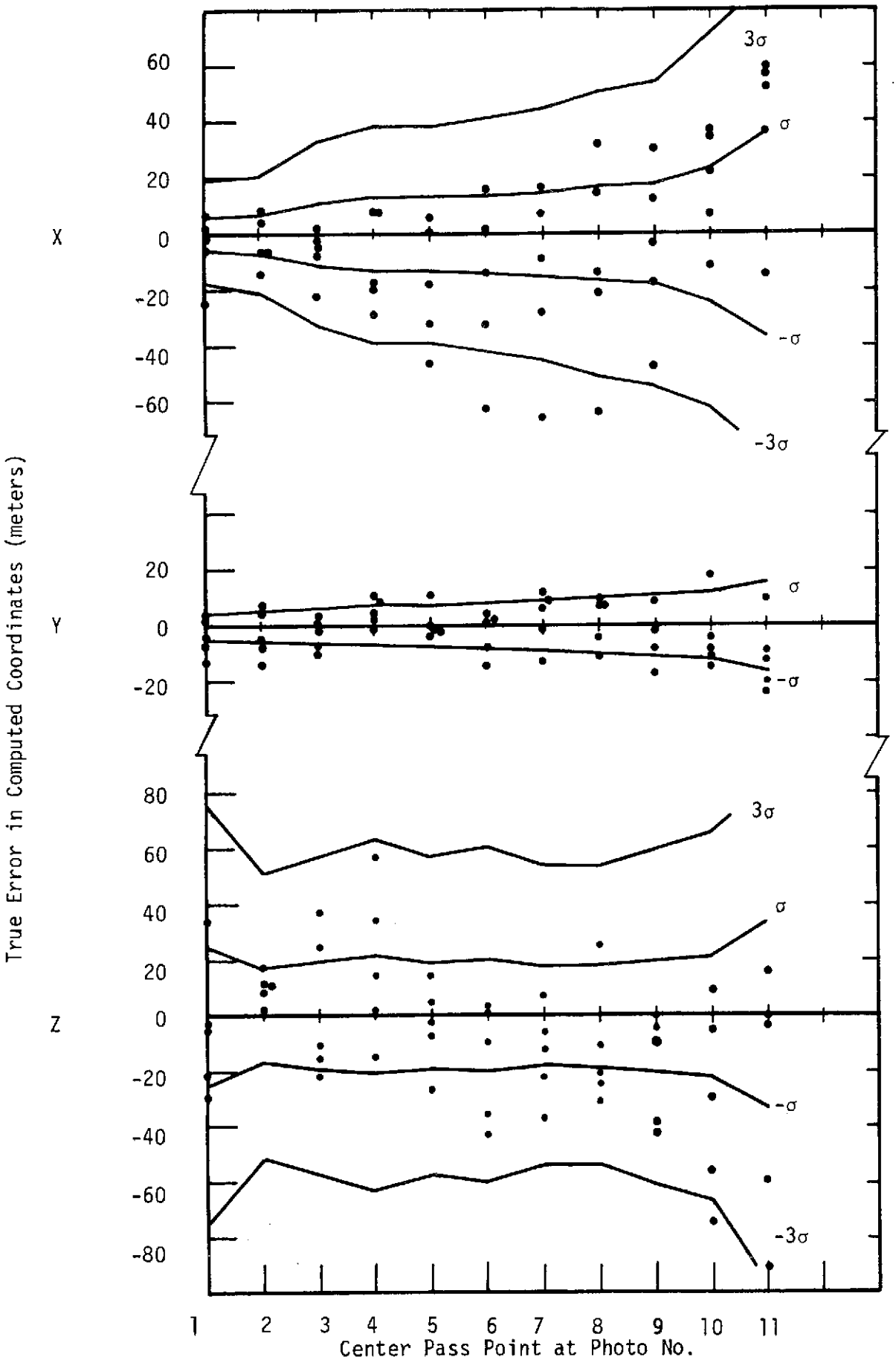

Fig. 4. True Error in Computed Pass Point Coordinates of Five Cases (Tracking + Attitude Controls)

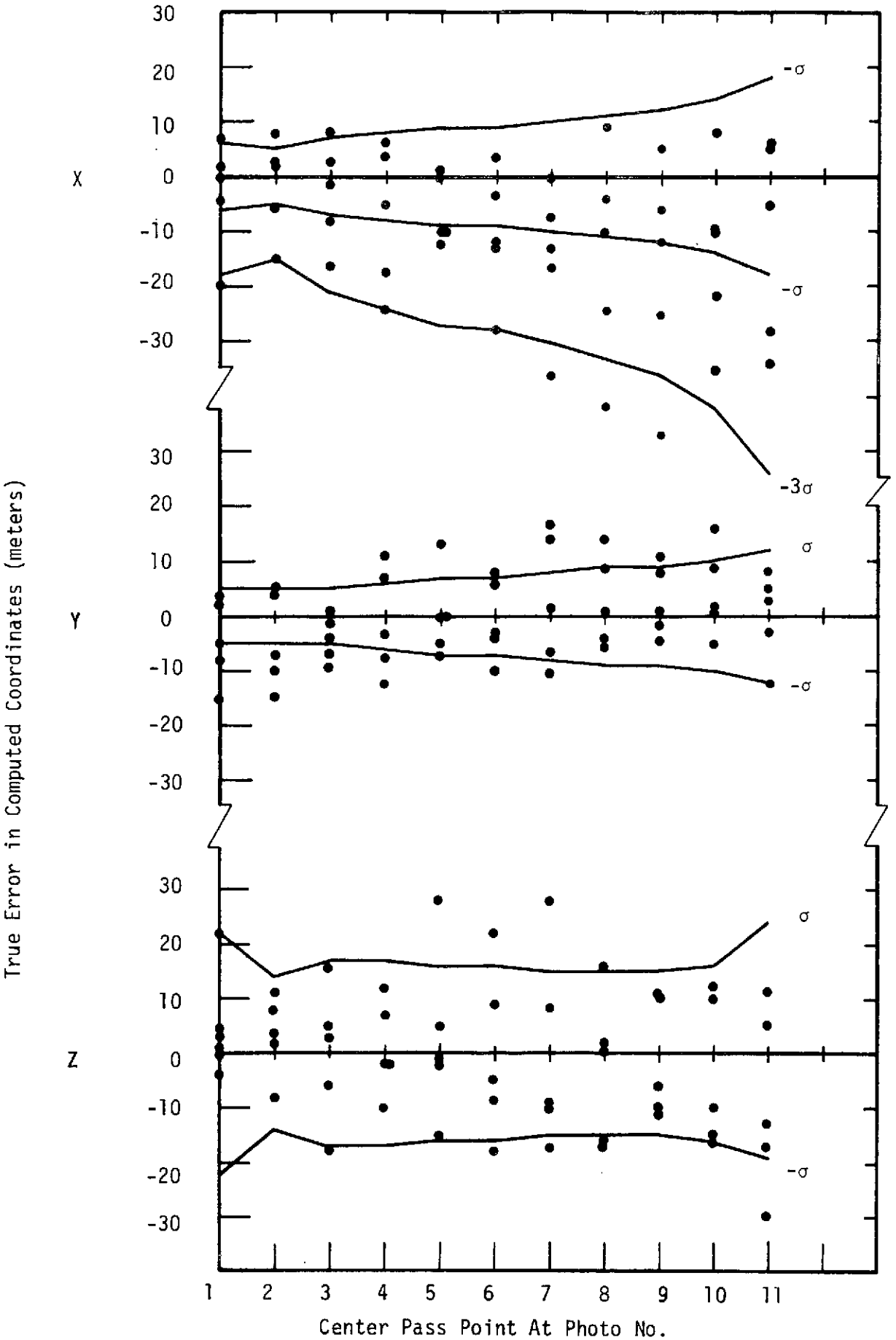

Fig. 5. True Error in Computed Pass Point Coordinates of Five Cases (Tracking + Altimeter + Attitude Controls)

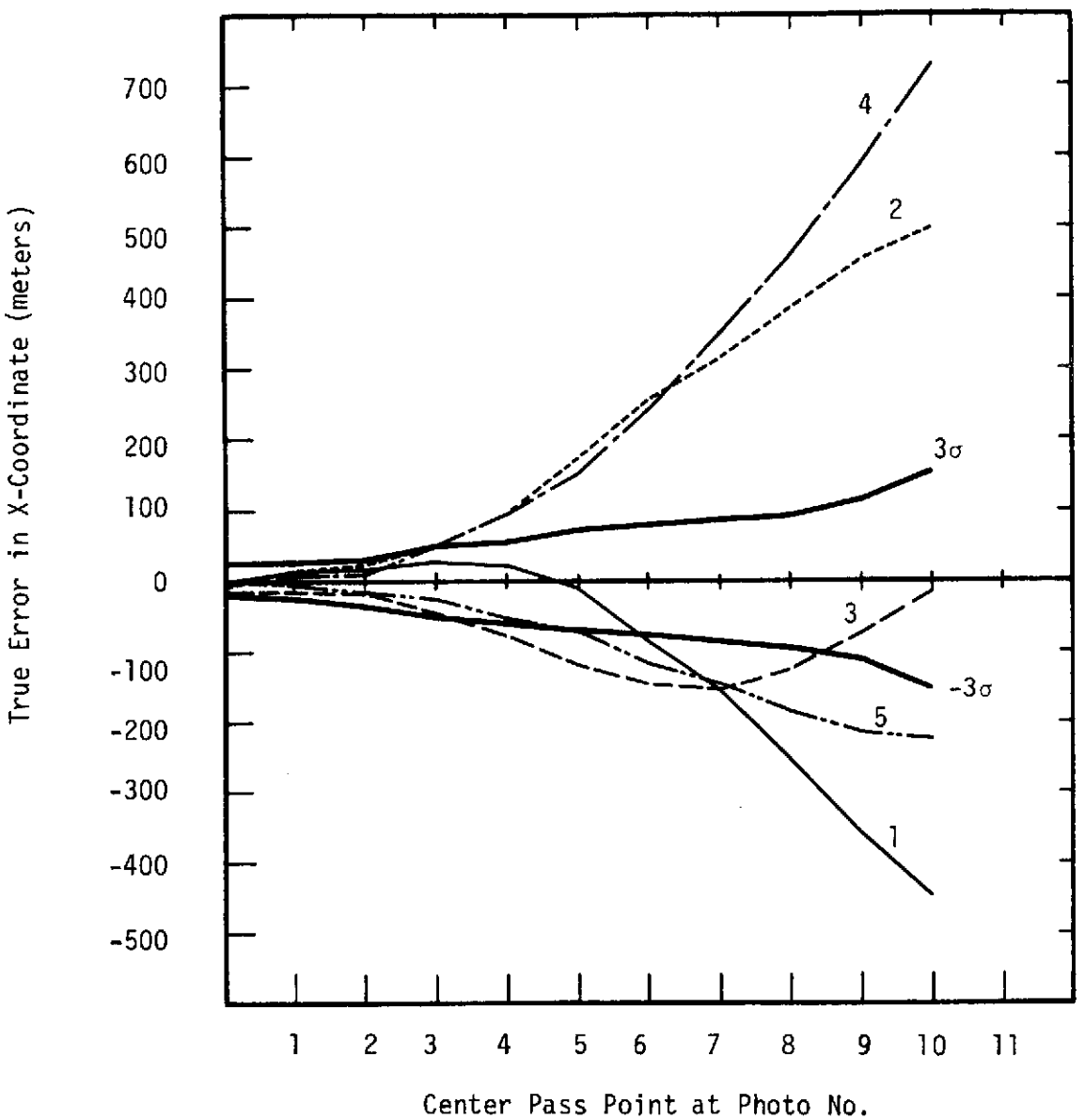

Fig. 6. True Error in X-Coordinate of Computed Pass Points (Cantilever Extension)

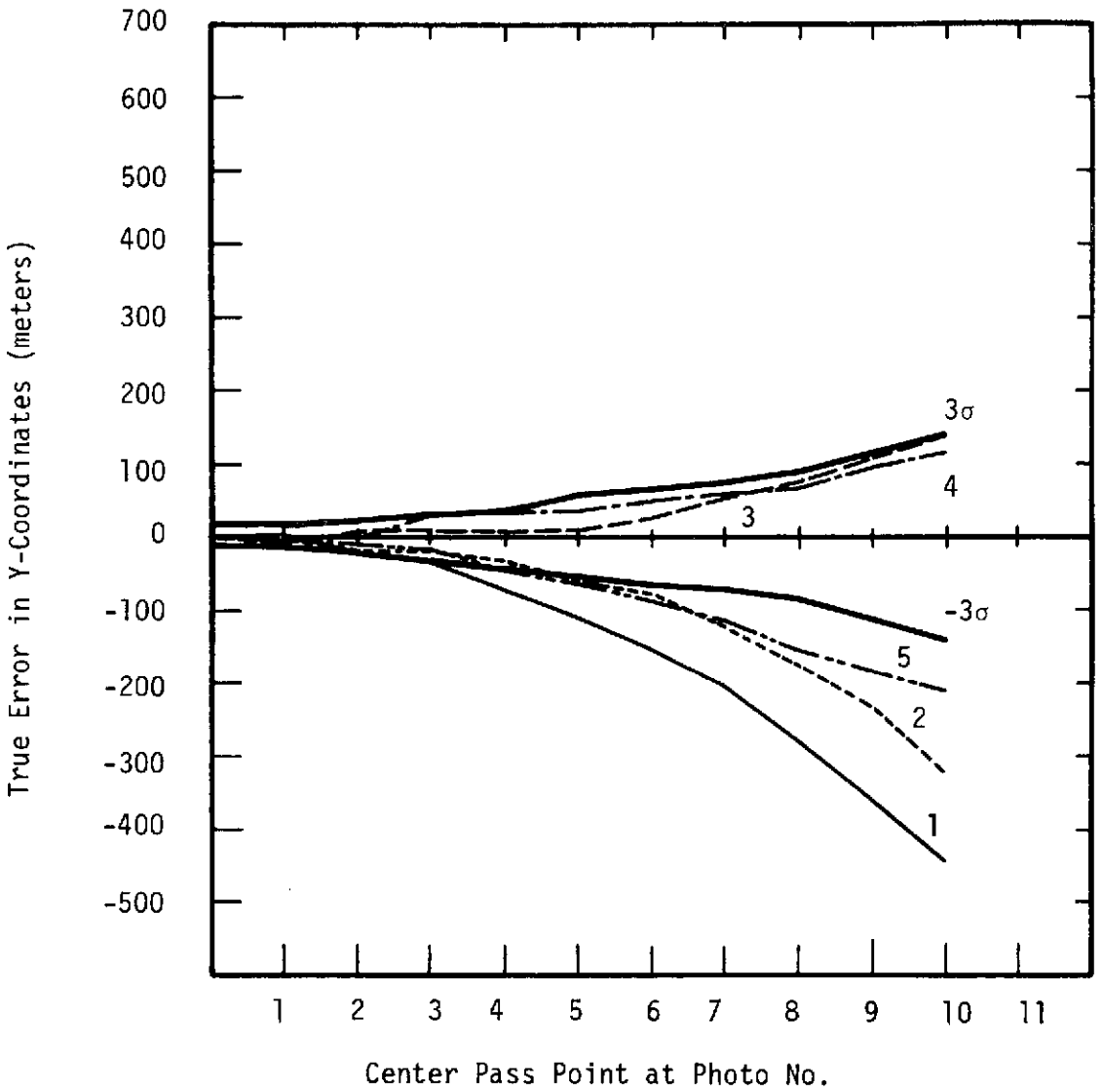

Fig. 7. True Error in Y-Coordinate of Center Pass Points (Cantilever Extension)

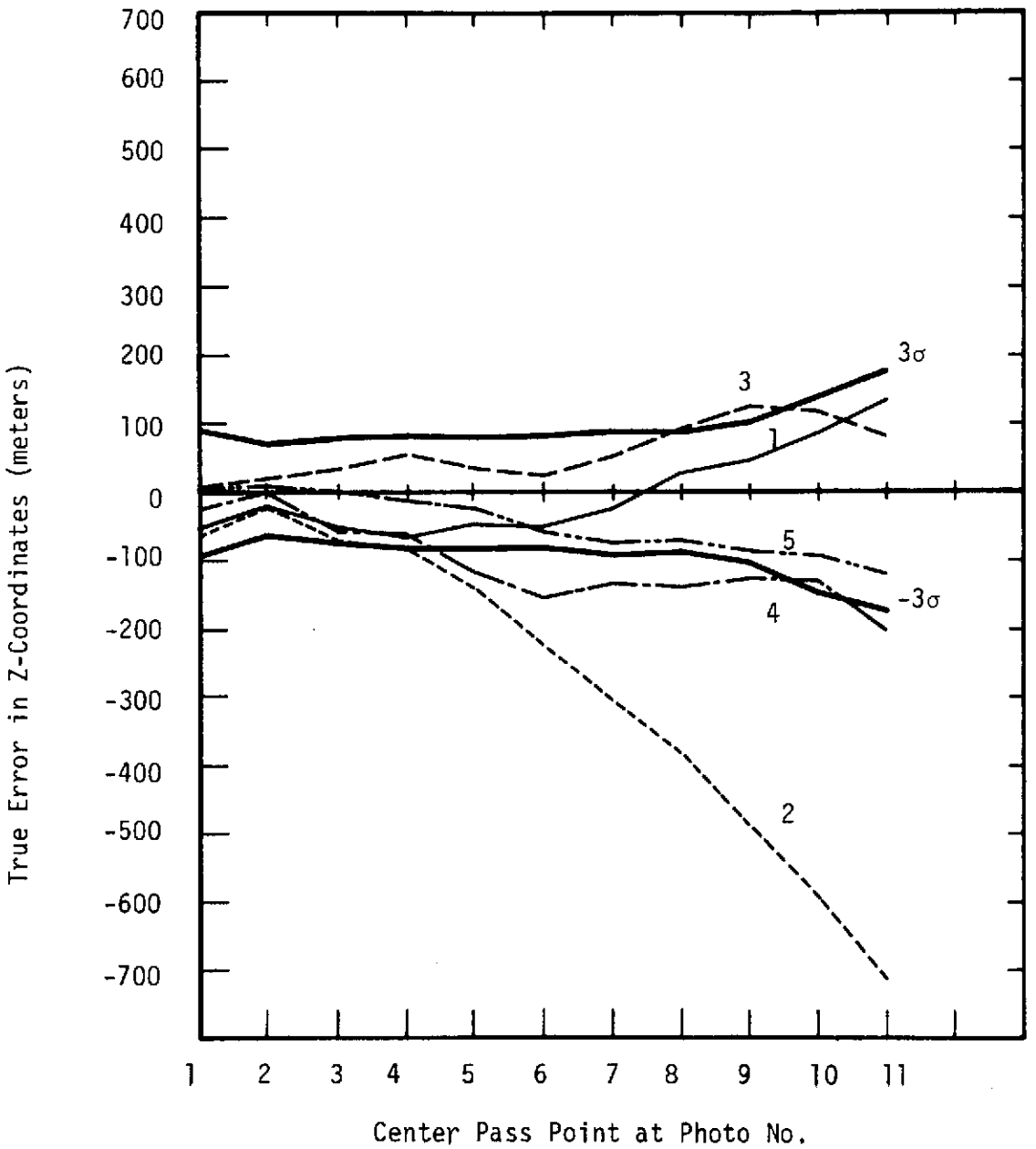

Fig. 8. True Error in Z-Coordinate of Center Pass Points (Cantilever Extension)

Table 2. Expected RMS Error vs. True Error in X-Coordinate of Exposure Stations (Tracking + Altimeter + Attitude Controls With $\sigma_V = \pm 0.5$ m./sec.)

Station	Expected RMS Errors (± meters)	True Error in Case (meters)					Last Correction in Case				
		1	2	3	4	5	1	2	3	4	5
1	-	-	-	-	-	-	-	-	-	-	-
2	10	-5	-10	4	26	-6	-3	-3	5	-6	1
3	11	+3	-13	1	6	6	-6	-3	6	-6	2
4	12	25	20	18	3	-10	-9	-2	5	-4	3
5	13	-1	-10	-19	-4	-6	-10	2	7	-8	2
6	13	-2	-32	-28	2	14	-10	6	7	-2	7
7	14	-7	-17	-31	2	21	-5	-2	4	-7	5
8	15	3	-14	-39	7	-4	-9	-6	8	-6	5
9	15	-16	-25	-36	9	-25	-11	-7	8	-9	0
10	16	-16	-11	-38	13	-33	-12	-3	10	-9	1
11	18	13	0	-36	17	-8	-9	-2	5	-7	0

Table 3. Expected RMS Error vs True Error in Y-Coordinates of Exposure Stations (Tracking + Altimeter + Attitude Controls With $\sigma_V = \pm 0.5$ m./sec.)

Station	Expected RMS Error (± meters)	True Error in Case					Last Correction in Case				
		1	2	3	4	5	1	2	3	4	5
		(meters)									
1	-	-	-	-	-	-	-	-	-	-	-
2	7	-14	4	-16	- 5	+ 3	-2	3	0	1.0	1
3	7	11	13	- 9	- 3	- 5	-4	2	0	0	1
4	8	4	11	4	-15	-13	-3	4	0	0	1
5	8	-17	5	- 9	-24	- 4	-5	3	0	-1	0
6	8	8	4	- 4	- 1	0	-5	5	0	-1	2
7	9	6	19	- 6	- 8	- 8	-4	5	0	-1	3
8	9	12	27	- 5	- 9	-16	-5	8	0	-1	3
9	10	1	19	- 1	-17	11	-6	8	0	0	3
10	11	2	16	16	-12	- 8	-5	10	1	-1	5
11	11	16	17	10	-15	4	-5	9	0	-2	4

Table 4. Expected RMS Error vs True Error in Z-Coordinates of Exposure Stations (Tracking + Altimeter + Attitude Controls With $\sigma_V = \pm 0.5$ m./sec.)

Station	Expected RMS Error (± meters)	True Error in Case					Last Correction in Case				
		1	2	3	4	5	1	2	3	4	5
		(meters)									
1	-	-	-	-	-	-	-	-	-	-	-
2	6	10	- 8	2	- 4	9	- 2	-	0	2	1
3	8	8	-20	- 6	2	0	- 4	- 1	0	3	- 3
4	9	13	-13	- 4	0	8	- 4	- 2	-2	3	- 5
5	9	23	-14	- 1	0	11	- 3	- 5	-2	5	- 8
6	10	23	-15	- 7	- 5	8	- 3	- 7	-3	5	-13
7	11	12	-19	- 9	- 6	13	- 5	-10	-2	4	-17
8	11	15	-19	-18	1	5	- 7	-10	-2	4	-20
9	12	11	-12	-14	-14	6	- 9	- 8	-4	5	-22
10	14	11	- 6	-18	-14	7	- 8	- 6	-4	8	-25
11	16	16	- 8	-21	-23	11	-12	- 5	-6	10	-24

Table 5. Expected RMS Error vs. True Error in X-Coordinates of Exposure Stations (Cantilever Extension)

Station	Expected RMS Error	True Error in Case					Last Correction in Case				
		1	2	3	4	5	1	2	3	4	5
		(meters)									
1	-	-	-	-	-	-	-	-	-	-	-
2	-	-	-	-	-	-	-	-	-	-	-
3	31	109	70	-19	- 18	- 5	16	-19	-15	47	- 1
4	37	100	79	61	-137	2	16	-34	26	17	- 6
5	35	74	-188	116	-184	12	7	-35	1	-19	-11
6	35	24	-356	171	-190	33	16	-13	-32	9	- 5
7	36	-105	-467	248	-231	93	33	- 7	-20	-19	- 2
8	37	-168	-553	244	-325	137	59	33	2	-15	0
9	37	-299	-573	169	-454	192	71	79	19	-43	- 3
10	43	-670	-637	111	-590	216	74	102	68	-83	- 6
11	59	-360	-667	- 4	-753	219	57	142	77	-103	-16

Table 6. Expected RMS Error vs. True Error in Y-Coordinates of Exposure Stations (Cantilever Extension)

Station	Expected RMS Error	True Error in Case					Last Correction in Case				
		1	2	3	4	5	1	2	3	4	5
		(meters)									
1	-	-	-	-	-	-	-	-	-	-	-
2	-	-	-	-	-	-	-	-	-	-	-
3	20	42	-15	-17	- 57	1	4	-16	- 6	21	- 5
4	26	- 8	-34	-28	- 92	27	5	-27	15	24	-10
5	30	- 92	-26	27	-127	61	- 4	-17	6	17	-17
6	29	-139	-35	10	-131	84	-16	-11	-21	24	-26
7	30	-187	-46	- 12	-127	107	-20	-12	-24	36	-34
8	30	-233	-13	- 40	-110	133	-30	- 1	-34	59	-50
9	32	-277	29	- 58	-113	160	-44	19	-25	38	-60
10	37	-391	77	- 52	-158	195	-52	4	-37	65	-81
11	46	-542	122	-103	-153	223	-37	58	-70	35	-99

Table 7. Expected RMS Error vs. True Error in Z-Coordinate of Exposure Stations (Cantilever Extension)

Station	Expected RMS Error	True Error in Case					Last Correction in Case				
		1	2	3	4	5	1	2	3	4	5
	(meters)										
1	-	-	-	-	-	-	-	-	-	-	-
2	-	-	-	-	-	-	-	-	-	-	-
3	12	- 36	21	27	-27	11	- 5	12	4	-15	5
4	19	- 71	11	29	1	34	- 5	21	-17	-16	11
5	22	- 85	23	17	15	58	0	27	-17	- 2	20
6	23	-104	87	- 1	7	85	2	34	- 3	- 9	31
7	23	-114	178	93	- 2	114	- 4	38	8	- 2	36
8	23	-101	285	- 91	-34	125	-14	28	22	4	39
9	26	77	381	-141	-17	124	-26	9	36	18	40
10	37	- 31	499	-168	- 7	128	-36	- 9	49	42	40
11	55	- 7	613	-149	27	140	-39	-55	65	93	45

3.3.3 Conclusions from experiments

Based on these experimental results, the following conclusions can be drawn:

1. In phototriangulation problems where only low-accuracy controls are available, the correction parameters generally will not reach zero in the iterative least-squares solution. However, the correction parameters should converge to a value less than the estimated RMS errors computed from the propagation of variance.
2. Generally, if controls are available throughout the strip or block (even though they are of low accuracy) and if the correction parameters converge to a value less than the computed RMS values, then the computed RMS values should be a good estimator for the accuracy of the computed parameters.
3. The RMS errors computed by the propagation of variance cannot detect the rapid accumulation of systematic effects from random errors. It is well known that the double-summation effect of random errors produce systematic errors in phototriangulation.
4. Generally, when the corrections in the last iteration exceed the computed RMS errors, then the RMS errors are not reliable as estimator of adjustment accuracy.

It is recommended that in simulation studies, true errors of the adjusted parameters should always be computed to check on the computed RMS error For problems in which the controls are sparsely distributed, several independent simulation cases should be performed to provide a check between the estimated RMS errors and the true errors.

3.4 Effectiveness of Various Control Data

The effectiveness of the three types of control data in improving the accuracy of lunar phototriangulation was studied by the propagation of variance. Three levels of tracking accuracy were assumed: $\pm$0.1, $\pm$0.5 and $\pm$1.0 m./sec. Altimeter measurements were assumed accurate to $\pm$3 m., and the attitude data were assumed to be accurate to $\pm$10 sec., $\pm$20 sec. and $\pm$10 sec. for ω, ϕ and κ respectively. For each level of tracking accuracy, the following combinations of control data were considered:

1) tracking alone;
2) tracking and altimeter;
3) tracking and attitude; and
4) tracking, altimeter and attitude.

Figures 9, 10 and 11 show the estimated RMS errors at the center pass points for the different combinations of controls at the three levels of tracking accuracy.

The results showed that the altimeter measurements mainly improved the accuracy in the X-coordinates of the pass points; while the attitude measurements improved the accuracy of the Y-coordinates. This result was anticipated because the altimeter measurement served primarily as scale control, while the attitude data served as direction control. Both types of control data were needed to achieve maximum accuracy in phototriangulation. Both the altimeter and attitude controls improve the elevation accuracy by about the same amount.

The cases in which all three types of controls were used are of particular interest. It can be concluded from Figures 9, 10 and 11 that for a single stereo model, the coordinates of the pass points can be determined with an RMS error of $\pm$7 m. in both X and Y and $\pm$15 m. in Z. At a tracking accuracy of $\pm$0.1 m./sec. for the velocity vector, there is practically no degradation of accuracy along the strip due to error propagation. At a tracking accuracy of $\pm$0.5 and $\pm$1.0 m./sec., the degradation in elevation accuracy along the strip is also negligible; but in both instances, the accuracy in the X- and Y- coordinates degenerates at the rate of about 1 m. and 0.5 m. per model respectively.

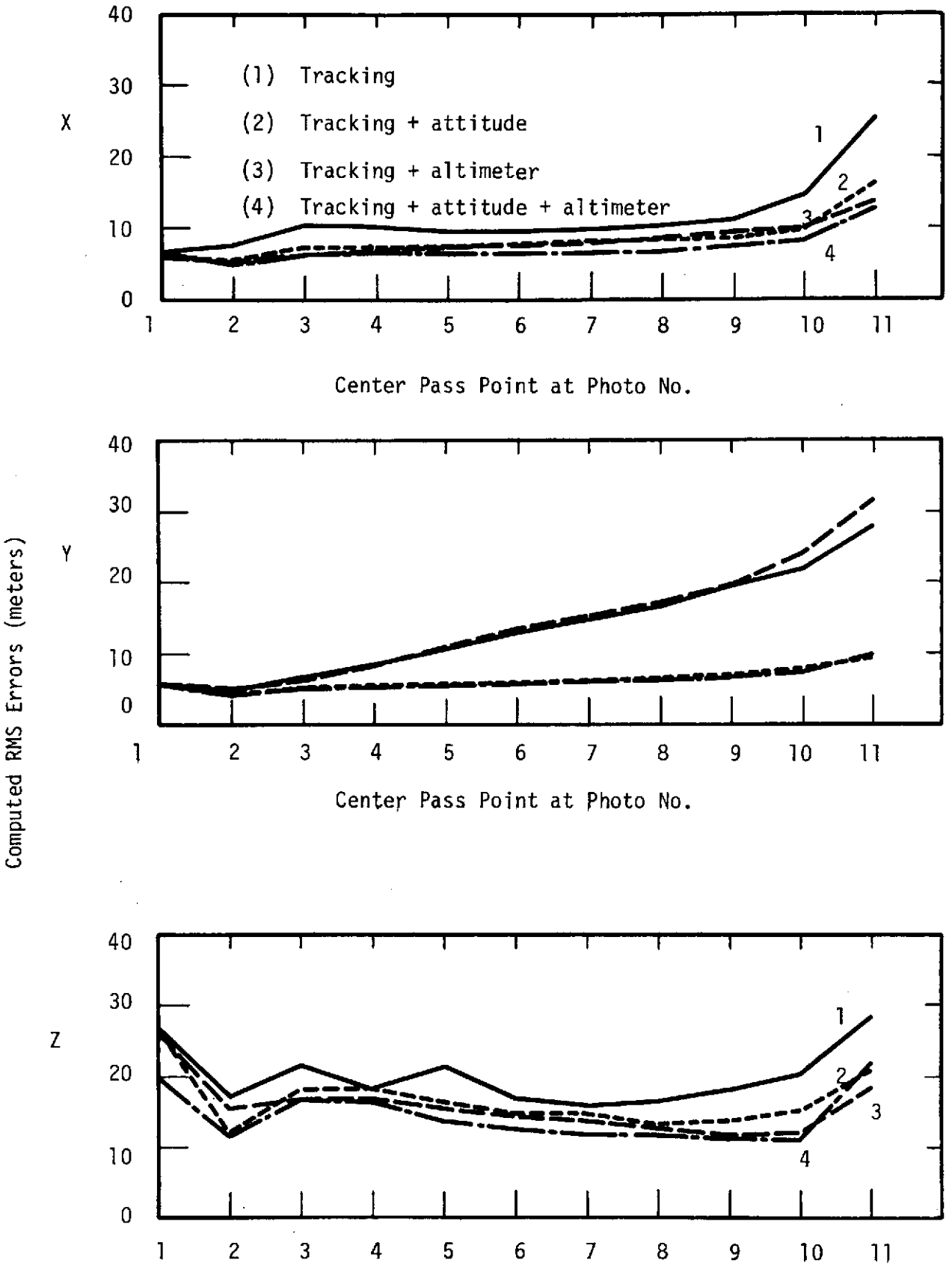

Fig. 9. Computed RMS Errors at Center Pass Points (Velocity Vector ±0.1 m./sec.)

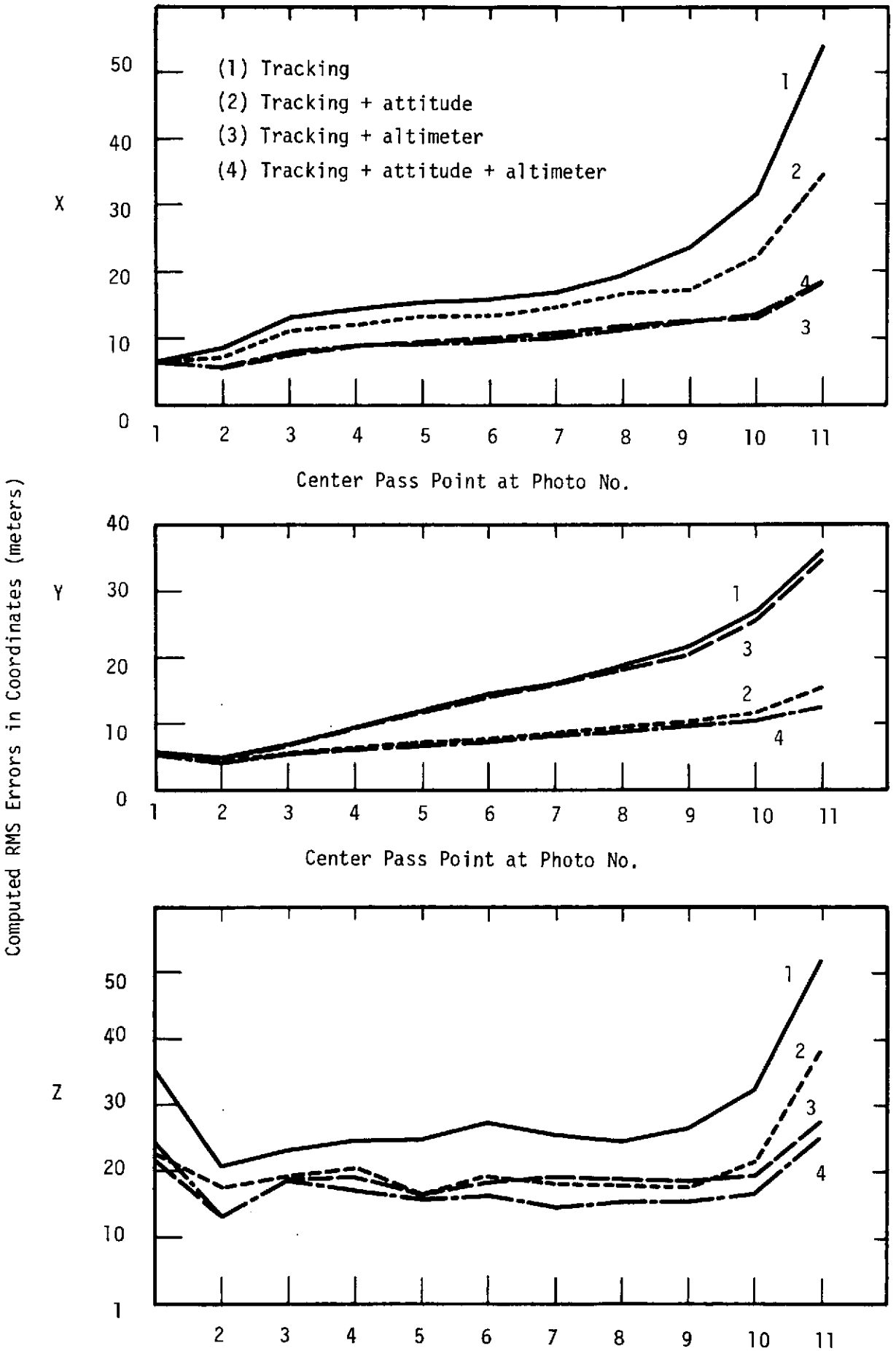

Fig. 10. Computed RMS Errors at Center Pass Points (Velocity Vector ±0.5 m./sec.)

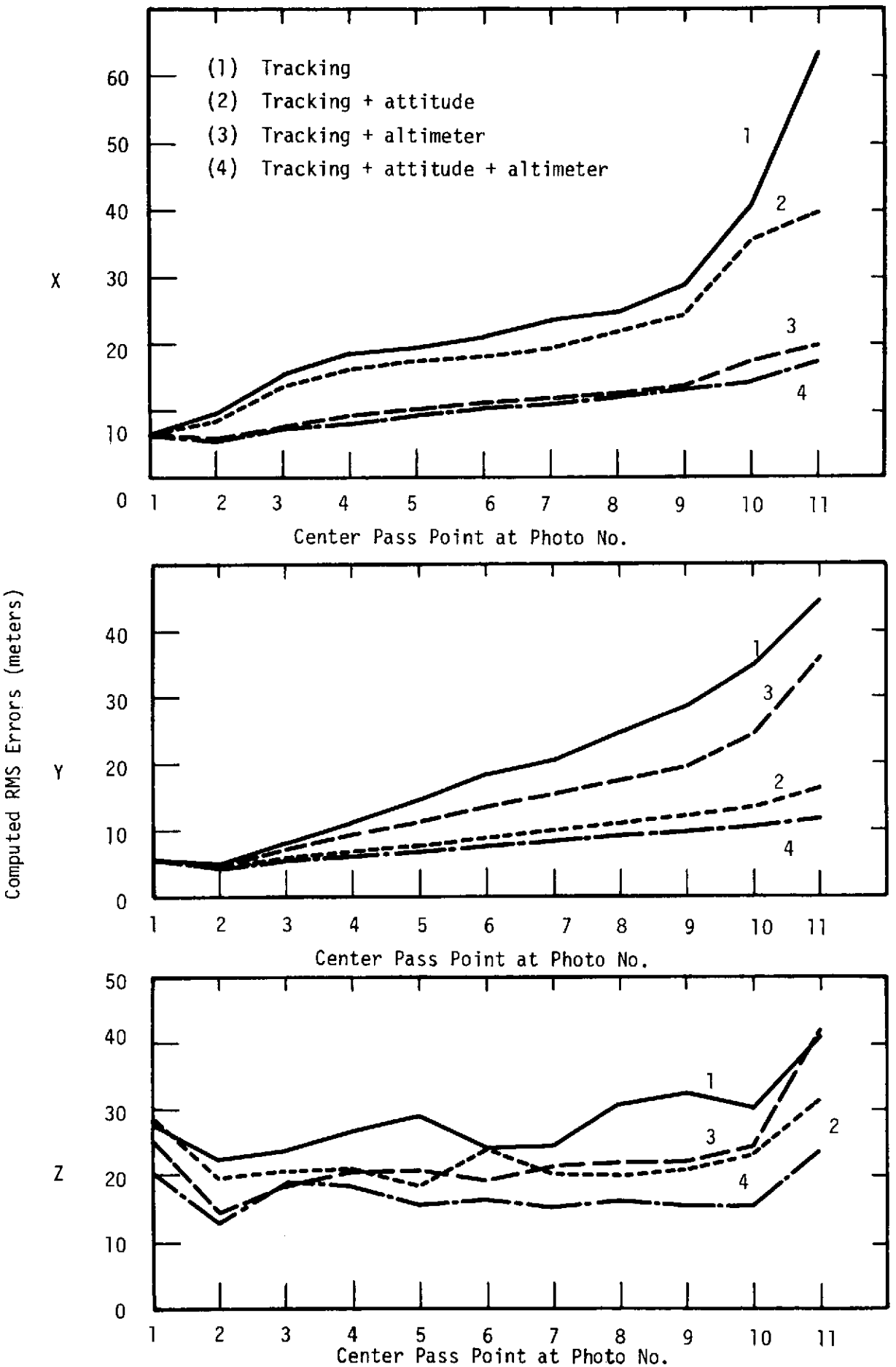

Fig. 11. Computed RMS Errors at Center Pass Points (Velocity Vector ±1.0 m./sec.)

4. ACCURACY ANALYSIS IN ABSOLUTE ORIENTATION

4.1 Compute Program THREED

The accuracy of absolute orientation depends on the following factors: 1) accuracy of the model coordinates; 2) accuracy of the ground controls, 3) density and distribution of control points, 4) size of the area, and 5) scale of the stereo model.

A computer program with complete error analysis capability has been developed for performing absolute orientation. The program is code named THREED. It may be used to perform any one of the following functions:

1. To perform absolute orientation.

The program takes as input the model coordinates of a set of model points and the ground coordinates of a group of control points. Both the model and the ground coordinates of the control points can be weighted individually according to their variance-covariance matrices. The program computes the seven transformation parameters (X_T, Y_T, Z_T, ω, ϕ, κ and scale) and their estimated standard errors. The program also transforms the model coordinates of any pass point in the ground reference system and determines the standard errors of the transformed coordinates.

2. To determine accuracy of absolute orientation by simulation.

In simulation application, the program takes as input 1) the ground coordinates of a set of control points; 2) the variances of the ground control coordinates; 3) the variances of the model coordinates; and 4) the scale of the model. The program then generates a set of model coordinates for the given ground points and perturbs them according to the specified accuracy of the model points. It then performs a regular absolute orientation solution and outputs the estimated standard errors of the seven absolute orientation parameters.

3. To determine the uncertainty in the orientation of a surface defined by a set of triangulated pass points.

The direct output of any phototriangulation solution is the ground coordinates of a set of pass points and their standard errors. Program THREED can be used to determine the uncertainty in the orientation (X_T, Y_T, Z_T, ω, ϕ, κ and scale) of the surface defined by the set of pass points.

A complete documentation of this program is being published separately (8).

4.2 Mathematical Formulation

The program THREED is based on the equations for three-dimensional conformal transformation which are as follows:

$$\begin{bmatrix} x_j \\ y_j \\ z_j \end{bmatrix} = \lambda \begin{bmatrix} m_{11} & m_{12} & m_{13} \\ m_{21} & m_{22} & m_{23} \\ m_{31} & m_{32} & m_{33} \end{bmatrix} \begin{bmatrix} X_j - X_T \\ Y_j - Y_T \\ Z_j - Z_T \end{bmatrix} \tag{4.1}$$

where

x_j, y_j, z_j model coordinates of point j

X_j, Y_j, Z_j ground coordinates of point j

X_T, Y_T, Z_T three translations

λ scale factor

$m_{11} = \cos\phi \cos\kappa$

$m_{12} = \cos\omega \sin\kappa + \sin\omega \sin\phi \cos\kappa$

$m_{13} = \sin\omega \sin\kappa - \cos\omega \sin\phi \cos\kappa$

$a_{21} = -\cos\phi \sin\kappa$

$a_{22} = \cos\omega \cos\kappa - \sin\omega \sin\phi \sin\kappa$

$a_{23} = \sin\omega \cos\kappa + \cos\omega \sin\phi \sin\kappa$

$a_{31} = \sin\phi$

$a_{32} = -\sin\omega \cos\phi$

$a_{33} = \cos\omega \cos\phi$

After linearization by first-order approximation, Eq. (4.1) may be expressed as follows:

$$\begin{bmatrix} V_{x_j} \\ V_{y_j} \\ V_{z_j} \end{bmatrix} + \begin{bmatrix} b_{11} & b_{12} & b_{13} & b_{14} & b_{15} & b_{16} & b_{17} \\ b_{21} & b_{22} & b_{23} & b_{24} & b_{25} & b_{26} & b_{27} \\ b_{31} & b_{32} & b_{33} & b_{34} & b_{35} & b_{36} & b_{37} \end{bmatrix} \begin{bmatrix} \Delta X_T \\ \Delta Y_T \\ \Delta Z_T \\ \Delta\omega \\ \Delta\phi \\ \Delta\kappa \\ \Delta\lambda \end{bmatrix} + \begin{bmatrix} d_{11} & d_{12} & d_{13} \\ d_{21} & d_{22} & d_{23} \\ d_{31} & d_{32} & d_{33} \end{bmatrix} \begin{bmatrix} \Delta X_j \\ \Delta Y_j \\ \Delta Z_j \end{bmatrix} = \begin{bmatrix} \varepsilon_{X_j} \\ \varepsilon_{Y_j} \\ \varepsilon_{Z_j} \end{bmatrix}$$

$$\text{i.e. } \dot{V}_j + \dot{B}_j\dot{\Delta} + \ddot{B}_j\ddot{\Delta}_j = \dot{\varepsilon}_j \qquad (4.2)$$

The model coordinates of each control point generates one set of equations as in Eq. (4.2). For m control points, the complete set of observation equations may be expressed as follows:

$$\begin{bmatrix} \dot{V}_1 \\ \dot{V}_2 \\ \cdot \\ \cdot \\ \dot{V}_m \end{bmatrix} + \begin{bmatrix} \dot{B}_1 \\ \dot{B}_2 \\ \cdot \\ \cdot \\ \dot{B}_m \end{bmatrix} \Delta + \begin{bmatrix} \ddot{B}_1 & & & \\ & \ddot{B}_2 & & \\ & & \cdot & \\ & & & \ddot{B}_m \end{bmatrix} \begin{bmatrix} \ddot{\Delta}_1 \\ \ddot{\Delta}_2 \\ \cdot \\ \cdot \\ \ddot{\Delta}_m \end{bmatrix} = \begin{bmatrix} \dot{\varepsilon}_1 \\ \dot{\varepsilon}_2 \\ \cdot \\ \cdot \\ \dot{\varepsilon}_m \end{bmatrix}$$

$$\text{i.e. } \dot{V} + \dot{B}\dot{\Delta} + \ddot{B}\ddot{\Delta} = \dot{\varepsilon} \qquad (4.3)$$

In order to permit flexible weighting of the seven transformation parameters as well as the ground control coordinates, one set of observation equations is introduced for each. The set of observation equations for the transformation parameters are as follows:

$$\ddot{V}_{X_T} - \Delta X_T = X_T^o - X_T^{oo}$$

$$\ddot{V}_{Y_T} - \Delta Y_T = Y_T^o - Y_T^{oo}$$

$$\ddot{V}_{Z_T} - \Delta Z_T = Z_T^o - Z_T^{oo}$$

$$\ddot{V}_{\omega} - \Delta\omega = \omega^o - \omega^{oo}$$

$$\ddot{V}_{\phi} - \Delta\phi = \phi^{o} - \phi^{oo}$$
$$\ddot{V}_{\kappa} - \Delta\kappa = \kappa^{o} - \kappa^{oo}$$
$$\ddot{V}_{\lambda} - \Delta\lambda = \lambda^{o} - \lambda^{oo}$$

where X_T^o, Y_T^o, ... and λ^o are approximated parameters; and X_T^{oo}, Y_T^{oo}, ... and λ^{oo} are measured parameters. In matrix notation, this set of equations may be simply written as follows:

$$\underset{(7,1)}{\ddot{V}} - \underset{(7,1)}{\dot{\Delta}} = \underset{(7,1)}{\ddot{\varepsilon}} \tag{4.4}$$

The observation equations for the jth ground control point are as follows:

$$\begin{bmatrix} \ddot{V}_{X_j} \\ \ddot{V}_{Y_j} \\ \ddot{V}_{Z_j} \end{bmatrix} - \begin{bmatrix} \Delta X_j \\ \Delta Y_j \\ \Delta Z_j \end{bmatrix} = \begin{bmatrix} X_j^o - X_j^{oo} \\ Y_j^o - Y_j^{oo} \\ Z_j^o - Z_j^{oo} \end{bmatrix} \tag{4.5}$$

Again, the superscript (o) denotes approximation parameters and the superscript (oo) denotes measured parameters. Equation (4.5) may be simply written as

$$\dddot{V}_j - \ddot{\Delta}_j = \dddot{\varepsilon}_j$$

The complete set of observation equations for all control points are as follows:

$$\begin{bmatrix} \ddot{V}_1 \\ \dddot{V}_2 \\ \cdot \\ \cdot \\ \cdot \\ \dddot{V}_m \end{bmatrix} - \begin{bmatrix} \ddot{\Delta}_1 \\ \ddot{\Delta}_2 \\ \cdot \\ \cdot \\ \cdot \\ \ddot{\Delta}_m \end{bmatrix} = \begin{bmatrix} \dddot{\varepsilon}_1 \\ \dddot{\varepsilon}_2 \\ \cdot \\ \cdot \\ \cdot \\ \dddot{\varepsilon}_m \end{bmatrix}$$

i.e. $$\dddot{V} - \ddot{\Delta} = \dddot{\varepsilon} \tag{4.6}$$

Combining Eqs. (4.3), (4.4) and (4.6) yields the following observation model:

$$\begin{bmatrix} \dot{V} \\ \ddot{V} \\ \dddot{V} \end{bmatrix} + \begin{bmatrix} \dot{B} & \ddot{B} \\ -I & 0 \\ 0 & -I \end{bmatrix} \begin{bmatrix} \dot{\Delta} \\ \\ \ddot{\Delta} \end{bmatrix} = \begin{bmatrix} \dot{\varepsilon} \\ \ddot{\varepsilon} \\ \dddot{\varepsilon} \end{bmatrix}$$

i.e. $$V + B\Delta = C \tag{4.7}$$

The normal equations is then as follows:

$$(B^T W B)\Delta = B^T W C \tag{4.8}$$

where W is the weight matrix for the observations. An iterative solution procedure must be followed. An initial set of approximate values is assigned to all unknown transformation parameters. The solution solved for the corrections and then apply the corrections to the approximations. The solution is iterated until a stable solution is reached.

After the last iteration, the variance-covariance matrix (σ_T) of the computed transformation parameters is computed by the following expression:

$$\sigma_T = \sigma_o^2 \, (B^T W B)^{-1} \tag{4.9}$$

where σ_o^2 is the variance of unit weight. The ground coordinates of all other model points and the corresponding standard errors are computed by the following expressions:

$$X_j = \frac{1}{\lambda} (m_{11} x_j + m_{21} y_j + m_{31} z_j) + X_T$$

$$Y_j = \frac{1}{\lambda} (m_{12} x_j + m_{22} y_j + m_{32} z_j) + Y_T$$

$$Z_j = \frac{1}{\lambda} (m_{13} x_j + m_{23} y_j + m_{33} z_j) + Z_T$$

$$\sigma_{X_j}^2 = (m_{11}x_j + m_{21}y_j + m_{31}z_j)^2\lambda^{-4}\sigma_{\lambda_j}^2$$
$$+ [-(\sin\phi\cos\kappa)x_j + (\sin\phi\sin\kappa)y_j + \cos\phi z_j]^2\lambda^{-2}\sigma_\phi^2$$
$$+ [-\cos\phi\sin\kappa x_j - \cos\phi\cos\kappa y_j]^2\lambda^{-2}\sigma_\kappa^2$$
$$+ m_{11}^2\lambda^{-2}\sigma_{X_j}^2 + m_{21}^2\lambda^{-2}\sigma_{Y_j}^2 + m_{31}^2\lambda^{-2}\sigma_{Z_j}^2 + \sigma_{X_T}^2$$

$$\sigma_{Y_j}^2 = (m_{12}x_j + m_{22}y_j + m_{32}z_j)^2\lambda^{-4}\sigma_{\lambda_j}^2$$
$$+ [(-\sin\omega\sin\kappa + \cos\omega\sin\phi\cos\kappa)x_j + (-\sin\omega\cos\kappa - \cos\omega\sin\phi\sin\kappa)y_j$$
$$- \cos\omega\cos\phi z_j]^2\lambda^{-2}\sigma_\omega^2$$
$$+ [(\sin\omega\cos\phi\cos\kappa)x_j - (\sin\omega\cos\phi\sin\kappa)y_j + \sin\omega\sin\phi z_j]^2\lambda^{-2}\sigma_\phi^2$$
$$+ [(\cos\omega\cos\kappa - \sin\omega\sin\phi\sin\kappa)x_j - (\cos\omega\sin\kappa + \sin\omega\sin\phi\cos\kappa)y_j]^2\lambda^{-2}\sigma_\kappa^2$$
$$+ m_{12}^2\lambda^{-2}\sigma_{X_j}^2 + m_{22}^2\lambda^{-2}\sigma_{Y_j}^2 + m_{32}^2\lambda^{-2}\sigma_{Z_j}^2 + \sigma_{Y_T}^2$$

$$\sigma_{Z_j}^2 = (m_{13}x_j + m_{23}y_j + m_{33}z_j)^2\lambda^{-4}\sigma_\lambda^2$$
$$+ [(\cos\omega\sin\kappa + \sin\omega\sin\phi\cos\kappa)x_j + (\cos\omega\cos\kappa - \sin\omega\sin\phi\sin\kappa)y_j$$
$$- \sin\omega\cos\phi z_j]^2\lambda^{-2}\sigma_\omega^2$$
$$+ [(-\cos\omega\cos\phi\cos\kappa)x_j + (\cos\omega\cos\phi\sin\kappa)y_j - \cos\omega\sin\phi z_j]^2\lambda^{-2}\sigma_\phi^2$$
$$+ [(\sin\omega\cos\kappa + \cos\omega\sin\phi\sin\kappa)x_j + (-\sin\omega\sin\kappa + \cos\omega\sin\phi\cos\kappa)y_j]^2\lambda^{-2}\sigma_\kappa^2$$
$$+ m_{13}^2\lambda^{-2}\sigma_{X_j}^2 + m_{23}^2\lambda^{-2}\sigma_{Y_j}^2 + m_{33}^2\lambda^{-2}\sigma_{Z_j}^2 + \sigma_{Z_T}^2 \qquad (4.10)$$

The m_{ij} terms in the above equations are defined as in Eq. (4.1).

4.3 Accuracy Analysis by Simulation

One major application of program THREED is the determination of absolute orientation accuracy by the method of simulation. Table 8 lists the simulation results for twenty-five cases in which the accuracy of the ground controls ranged between 1 km. and 2 km. The standard errors of the model coordinates ranged between 2 and 200 meters. The dimension of the square area ranged between 2 and 2000 km., while the scale of the model varied from 0.4 to 1.2. In all cases, the area was assumed to have twenty-five control points arranged in a 5 by 5 rectangular array.

Based on the results of these twenty-five cases, an unsuccessful attempt was made to develop a prediction equation for each of the transformation parameters. The following general polynomials was used in a regression analysis:

$$\sigma = a_0 + a_1\sigma_{XYZ} + a_2\sigma_{xyz} + a_3A + a_4S + a_5\sigma_{XYZ}^2 + a_6\sigma_{xyz}^2 + a_7A^2 + a_8S^2 \tag{4.11}$$

where

σ_{XYZ} standard errors of ground control coordinates

σ_{xyz} standard errors of model coordinates

A area

S scale

The coefficients a_0, a_1, ... and a_8 were determined in a regression analysis using the data in Table 8. Although excellent fit was obtained for the translation parameters (σ_{X_T}, σ_{Y_T}, and σ_{Z_T}), errors in the predicted accuracy of the rotational parameters (σ_ω, σ_ϕ, and σ_κ) generally exceeded $\pm 1°$.

Furthermore, Eq. (4.11) gives no consideration to the density and distribution of ground controls, which, are important factors governing the accuracy of absolute orientation.

Program THREED should provide the best means for evaluating absolute orientation accuracy.

Table 8. Accuracy of Absolute Orientation

$\sigma_{X,Y,Z}$ (meters)	$\sigma_{x,y,z}$ (meters)	Dimension of Square Area (km)	Model Scale	Standard Error of Absolute Orientation Parameters						
				Scale	X_T (meters)	Y_T (meters)	Z_T (meters)	ω ° ' "	ϕ ° ' "	κ ° ' "
1000	20	200	0.8	.0013	174	174	174	0- 8-55	0- 6-57	0- 7- 0
1250	6	20	0.6	.012	219	219	219	1-48-51	1-24-54	1-29-31
1250	6	20	1.0	.020	217	217	217	1-47-59	1-23-53	1-28-33
1250	6	2000	0.6	.0001	218	218	218	0-01-07	0- 0-52	0- 0-52
1250	6	2000	1.0	.0002	216	216	216	0-01-07	0- 0-53	0- 0-52
1250	63	20	0.6	.012	217	217	217	1-48-37	1-24-38	1-29-07
1250	63	20	1.0	.021	218	218	218	1-48-52	1-24-56	1-29-30
1250	63	2000	0.6	.0001	216	216	216	0- 1-07	0- 0-52	0- 0-52
1250	63	2000	1.0	.0002	217	217	217	0- 1-07	0- 0-52	0- 0-52
1750	6	20	0.6	.017	305	305	305	2-31-01	1-59-13	2-05-04
1750	6	20	1.0	.027	296	296	297	2-25-31	1-53-03	1-58-34
1750	6	2000	0.6	.00017	304	304	304	0-01-33	0-01-13	0-01-13
1750	6	2000	1.0	.00028	295	295	295	0-01-34	0-01-13	0-01-13
1750	63	20	0.6	.018	305	305	305	2-32-20	1-59-56	2-05-14
1750	63	20	1.0	.029	305	305	305	2-31-28	1-59-47	2-04-47
1750	63	2000	0.6	.00017	303	303	303	0- 1-33	0- 1-13	0- 1-13
1750	63	2000	1.0	.00028	304	304	305	0- 1-34	0- 1-13	0- 1-13
1500	20	200	0.4	.001	261	261	261	0-13-21	0-10-26	0-10-29
1500	20	200	1.2	.003	261	261	261	0-13-22	0-10-26	0-10-29
1500	20	2	0.8	.12	275	278	274	10-21-52	10-48-23	15-48-47
1500	20	2000	0.8	.00002	261	261	262	0- 0- 8	0- 0- 6	0- 0- 6
1500	2	200	0.8	.0017	244	256	250	0-11-54	0-09-34	0-09-27
1500	200	200	0.8	.0019	260	260	260	0-13-21	0-10-26	0-10-28
1500	20	200	0.8	.0019	261	261	261	0-13-23	0-10-27	0-10-29
2000	20	200	0.8	.0026	348	348	349	0-17-49	0-13-56	0-13-59

4.4 Analysis of Apollo 15 Data

Program THREED was used to evaluate the mapping accuracy of the Apollo 15 photography. Figure 12 shows the overlapping coverage between a stereoscopic model of the 76 mm. metric photography and three successive stereoscopic models of panoramic photography.

The stereoscopic model of 76-mm. metric photography was absolutely oriented on the AS-11-B1 using orientation parameters derived from tracking and stellar camera data. The ground coordinates of the model points in Fig. 12 were measured directly from the model in the AS-11-B1. Table 9 presents a listing of these ground coordinates.

The three panoramic stereomodels were also individually oriented in the AS-11-B1. The model coordinates of the control points as well as about 20 other model points were recorded. To minimize the errors introduced by the geometry of the panoramic photography, only the central 17.5° sweep portion of each frame ($\pm$8.25° from center) was used. Tables 10, 11 and 12 list the model coordinates for the three panoramic stereo models.

All the above AS-11-B1 measurements were performed by Lockheed Electronics Company, at the NASA Johnson Space Center, Houston.

Program THREED was used to perform absolute orientation of the panoramic models and to perform error analysis. After several trial solutions, the following sets of standard errors for both the model and the ground coordinates were found to give the best agreement between the computed standard error of unit weight and the predefined value;

Model Coordinates	Ground Coordinates
$\sigma_x = \pm$ 0.010 mm.	$\sigma_X = \pm$ 15 m.
$\sigma_y = \pm$ 0.010 mm.	$\sigma_Y = \pm$ 10 m.
$\sigma_z = \pm$ 0.010 mm.	$\sigma_Z = \pm$ 25 m.

Table 13 lists the standard errors computed by program THREED for both the transformation parameters and the adjusted ground coordinates.

It can be concluded from this study that the ground coordinates derived from this procedure have the following relative positional accuracy within the 76-mm. stereo model: $\sigma_X = \pm 15$ m., $\sigma_Y = \pm 10$ m. and $\sigma_Z = \pm 25$ m. The orientation accuracy of the panoramic stereo models can be expected to be ± 3 minutes of arc in the ω and κ rotations and ± 7 min. in the ϕ rotation.

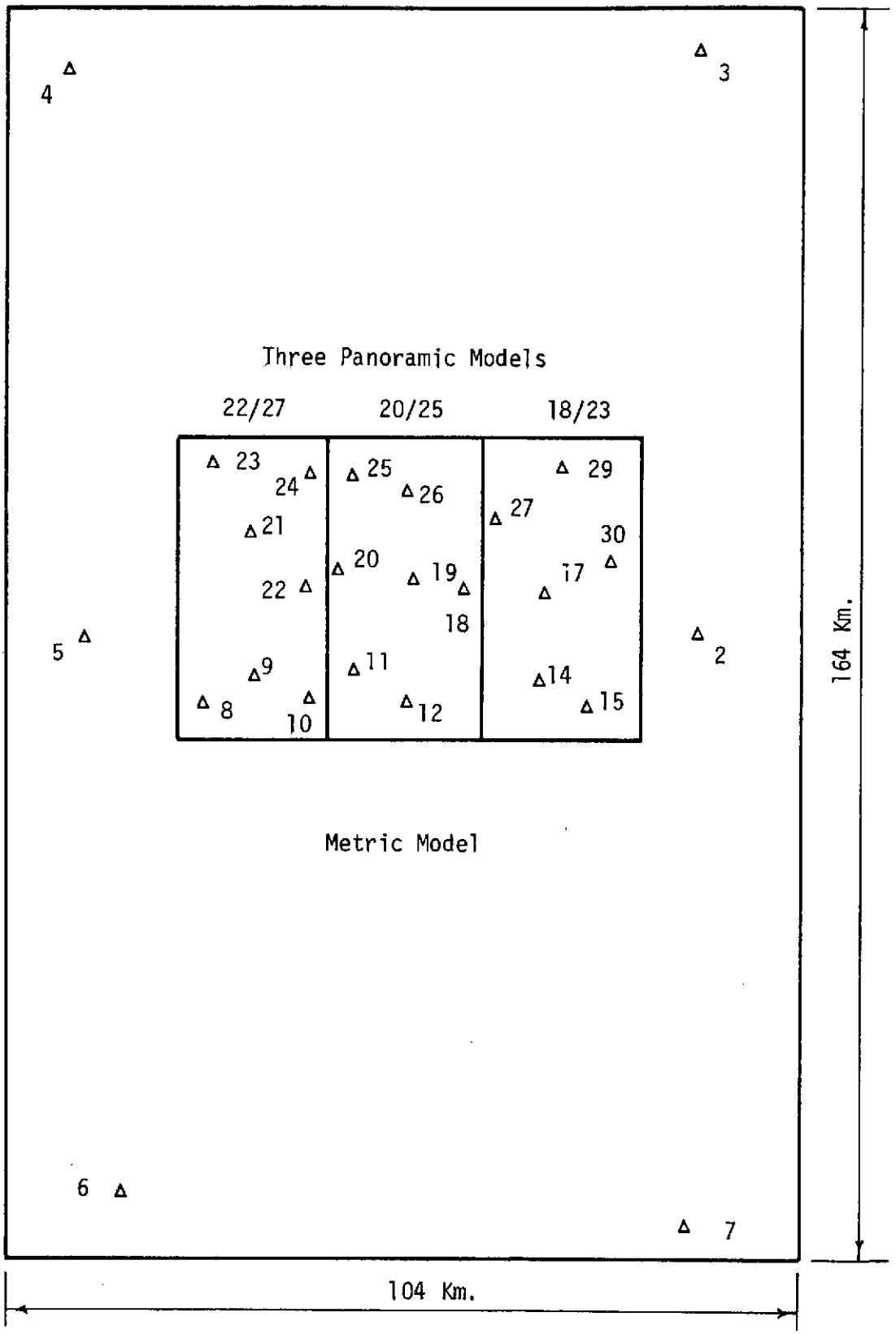

Fig. 12. Stereoscopic Coverage at One Metric Model and Three Panoramic Models

Table 9. Ground Coordinates Derived From the Metric Model

GROUND COORDINATES

POINT	X	Y	Z
8	-36497.0000	-9117.0000	232.0000
9	-29682.0000	-5536.0000	377.0000
10	-22551.0000	-8501.0000	422.0000
21	-30412.0000	13031.0000	372.0000
22	-22827.0000	6572.0000	203.0000
23	-35327.0000	22215.0000	1182.0000
24	-22453.0000	21101.0000	295.0000
11	-16923.0000	-4820.0000	1006.0000
12	-9550.0000	-9020.0000	476.0000
25	-17108.0000	20788.0000	338.0000
26	-9752.0000	18863.0000	326.0000
19	-9076.0000	6880.0000	471.0000
20	-19326.0000	8844.0000	133.0000
18	-2361.0000	5845.0000	305.0000
27	1806.0000	15096.0000	310.0000
29	10759.0000	21624.0000	386.0000
15	14080.0000	-9575.0000	904.0000
14	8007.0000	-6116.0000	360.0000
17	8701.0000	5200.0000	301.0000
30	17232.0000	9647.0000	347.0000

Table 10. Model Coordinates from Panoramic Model 22/27

MODEL COORDINATES

1. CONTROL POINTS

NUMBER	POINT	X	Y	Z
1	8	-36.8500	-99.3960	1.8360
2	9	9.0820	-76.4540	2.4760
3	10	56.3500	-96.8570	2.6570
4	21	6.0890	47.5630	2.4370
5	22	55.5340	3.6140	1.4570
6	23	-25.5300	109.1990	7.8360
7	24	59.9810	100.4220	2.2830

2. UNKNOWN POINTS

NUMBER	POINT	X	Y	Z
8	126	-38.0220	-17.8710	2.3150
9	118	-2.4400	-18.2550	3.0560
10	110	28.1510	-17.7480	2.3440
11	103	63.5470	-17.3580	1.4810
12	102	62.5500	19.5060	1.2460
13	109	32.3130	21.0880	2.4340
14	117	-0.8240	20.4110	2.6310
15	125	-36.9070	20.1300	2.5790
16	124	-39.3250	49.6360	2.2550
17	108	29.2470	51.8240	2.3590
18	101	61.7860	53.9560	2.2960
19	107	32.2640	90.2580	2.7140
20	115	-2.0260	87.3500	4.1060
21	123	-35.3630	87.5960	2.6990
22	122	-36.4530	115.8250	7.9560
23	106	28.5890	118.6400	2.7150
24	127	-33.7020	-44.6800	2.3020
25	119	-3.5830	-50.3710	4.1170
26	111	40.7050	-48.0320	6.0890
27	104	65.3890	-47.8490	4.3590
28	105	64.3700	-85.4150	4.9000
29	112	36.4960	-83.3250	2.8670
30	120	-2.0950	-69.6810	2.7150
31	128	-35.1640	-77.9410	2.0910

Table 11. Model Coordinates From Panoramic Model 20/25

MODEL COORDINATES

1. CONTROL POINTS

NUMBER	POINT	X	Y	Z
1	11	-37.9920	-74.6960	-2.1410
2	12	10.6850	-103.1930	-5.5940
3	25	-37.4780	96.1670	-6.7080
4	26	11.5460	82.7240	-6.8140
5	19	15.0690	2.6830	-5.6740
6	20	-53.2620	16.7970	-7.8810
7	18	59.7380	-4.6610	-6.9810

2. UNKNOWN POINTS

NUMBER	POINT	X	Y	Z
8	130	-43.3800	110.1420	-6.6990
9	136	-8.4390	112.9540	-6.4160
10	144	25.6170	116.5010	-6.2930
11	152	59.1410	111.1150	-6.2430
12	154	59.6470	40.5940	-6.5840
13	146	24.7540	50.9030	-6.3250
14	138	-6.1570	56.0330	-6.6140
15	131	-43.7580	45.3210	-8.0040
16	132	-43.7830	10.4920	-7.8070
17	139	-6.9850	17.9130	-6.7400
18	147	31.3370	21.2860	-6.3660
19	155	58.6940	10.7360	-6.4890
20	156	59.9080	-22.9870	-6.6030
21	148	27.6720	-30.3710	-6.1090
22	140	-3.7810	-21.7520	-6.6150
23	133	-38.9030	-22.8870	-7.8320
24	134	-42.6850	-49.6090	-6.1500

Table 12. Model Coordinates From Panoramic Model 18/23

MODEL COORDINATES

1. CONTROL POINTS

NUMBER	POINT	X	Y	Z
1	27	-45.3060	58.3960	-0.7990
2	29	14.9640	100.8650	-0.0610
3	15	33.9300	-107.6350	3.1330
4	14	-6.4020	-83.6530	-0.2150
5	17	-0.4790	-8.4340	-0.7040
6	30	56.8220	20.2310	-0.3620

2. UNKNOWN POINTS

NUMBER	POINT	X	Y	Z
7	2	49.5940	36.1320	3.4940
8	28	-38.4190	106.5860	-0.4200
9	175	-8.0570	-122.2780	0.2750
10	182	19.1600	-117.1890	3.0960
11	190	56.6780	-115.5610	4.2270
12	181	19.5660	-84.5990	1.9580
13	174	-10.9570	-88.4420	-0.3510
14	166	-42.5250	-86.6240	-0.2290
15	172	-10.2560	-21.7630	-0.5830
16	173	-13.2660	-57.2540	-0.3670
17	180	20.1330	-50.1900	0.0560
18	188	57.1720	-55.8450	2.1830
19	169	-9.5530	72.5150	-0.1700
20	177	20.3240	75.1330	-0.1280
21	184	54.6090	76.3210	3.1110
22	185	58.5690	47.8650	2.9140
23	178	26.0900	52.0830	0.0280
24	170	-10.6850	51.4980	-0.2360
25	163	-41.6560	5.0400	-0.6790
26	171	-5.2450	18.6590	-0.1260
27	186	54.8420	13.6500	-0.2230
28	187	53.0320	-14.1090	0.5070
29	199	28.9790	-23.7330	-1.1820
30	168	-11.2190	108.8190	-0.0410
31	183	58.2960	112.7730	2.5850
32	217	23.8970	110.4950	0.3390

Table 13. Accuracy in the Absolute Orientation of the Panoramic Models

Parameters		Panoramic Model 18/23	20/25	22/27
Predefined σ_o		$\pm$0.01 mm.	$\pm$0.01 mm.	$\pm$0.01 mm.
Computed σ_o		0.012 mm.	0.010 m.	0.012 mm.
σ_{X_T}		7 m.	6 m.	7 m.
σ_{Y_T}		5 m.	4 m.	5 m.
σ_{Z_T}		13 m.	9 m.	12 m.
σ_ω		3' 53"	3' 4"	3' 2"
σ_ϕ		8' 47"	5' 36"	6' 49"
σ_κ		1' 54"	1' 25"	1' 32"
σ_X	Adjusted Control	10 m.	9 m.	10 m.
σ_Y	Coordinates	8 m.	6 m.	8 m.
σ_Z		25 m.	18 m.	23 m.
σ_X	Transformed	13 m.	9 m.	11 m.
σ_Y	Model Coordinates	10 m.	7 m.	8 m.
σ_Z		32 m.	22 m.	26 m.
No. of Control Points Used in Solution		6	7	7

5. SLOPE ACCURACY

5.1 Error Propagation Formula

Let D be the horizontal distance between points i and j which have elevation h_i and h_j respectively. Then, the slope angle from point i to point j can be computed by the expression

$$S_{ij} = \tan^{-1}\left(\frac{h_j - h_i}{D}\right) = \tan^{-1}\left(\frac{\Delta h}{D}\right) \tag{5.1}$$

Hence, by the law of propagation of random errors, the standard error of the slope may be expressed as follows:

$$\sigma_{S_{ij}}^2 = \left(\frac{\partial S_{ij}}{\partial \Delta h}\right)^2 \sigma_{\Delta h}^2 + \left(\frac{\partial S_{ij}}{\partial D}\right)^2 \sigma_D^2 \tag{5.2}$$

Since

$$\frac{\partial S_{ij}}{\partial \Delta h} = \left(1 + \left(\frac{\Delta h}{D}\right)^2\right)^{-1} \frac{1}{D}$$

and $$\frac{\partial S_{ij}}{\partial D} = \left(1 + \left(\frac{\Delta h}{D}\right)^2\right)^{-1} \left(-\frac{\Delta h}{D^2}\right),$$

$$\sigma_{S_{ij}}^2 = \left[1 + \left(\frac{\Delta h}{D}\right)^2\right]^{-2} \cdot \left[\frac{1}{D^2}\sigma_{\Delta h}^2 + \left(\frac{\Delta h}{D^2}\right)^2 \sigma_D^2\right] \tag{5.3}$$

Assuming that $\sigma_{h_i} = \sigma_{h_j} = \sigma_h$;

then

$$\sigma_{\Delta h}^2 = 2\sigma_h. \tag{5.4}$$

Furthermore, since $D = [(X_j - X_i)^2 + (Y_j - Y_i)^2]^{1/2}$

$$\sigma_D^2 = D^2\{(X_j - X_i)^2 \sigma_{X_j}^2 + (Y_j - Y_i)^2 \sigma_{Y_j}^2 + (X_j - X_i)^2 \sigma_{X_i}^2 + (Y_j - Y_i)^2 \sigma_{Y_i}^2\}$$

Assuming that

$$\sigma_{X_j} = \sigma_{Y_j} = \sigma_{X_i} = \sigma_{Y_i} = \sigma_{X,Y},$$

then $$\sigma_D^2 = D^2\{2D^2\}\ \sigma_{X,Y}^2$$

i.e. $$\sigma_D^2 = 2\sigma_{X,Y}^2$$

Substituting Eqs. (5.4) and (5.5) into Eq. (5.3) yields

$$\sigma_{S_{ij}} = \sqrt{2}\ [1 + (\frac{h}{D})^2]^{-1}\ [\frac{1}{D^2}\ \sigma_h^2 + (\frac{\Delta h}{D^2})^2\ \sigma_{X,Y}^2]^{1/2} \qquad (5.6)$$

in which $\sigma_{S_{ij}}$ is given in radians. In general, Eq. (5.6) may be rewritten as follows:

$$\sigma_{S_{ij}} = c\ [1 + (\frac{\Delta h}{D})^2]^{-1}\ [\frac{1}{D^2}\ \sigma_h^2 + (\frac{\Delta h}{D^2})^2\ \sigma_{X,Y}^2]^{1/2} \qquad (5.7)$$

where c = 1.414 for $\sigma_{S_{ij}}$ in radians;

= 81.016 for $\sigma_{S_{ij}}$ in degrees;

= 4861 for $\sigma_{S_{ij}}$ in minutes;

= 2.916×10^5 for $\sigma_{S_{ij}}$ in seconds.

When D is much greater than Δh, the term for $\sigma_{X,Y}^2$ may be neglected resulting in the following simplified expression:

$$\sigma_{S_{ij}} = \pm\ \frac{c}{D[1 + (\frac{\Delta h}{D})^2]}\ \sigma_h \qquad (5.8)$$

5.2 Application on the Apollo 15 Data

Table 14 lists the THREED output ground coordinates for all pass points in the panoramic model 22/27. Table 15 lists the RMS errors in slopes along two profiles in this model. In all instances, the term $(\frac{\Delta h}{D^2})^2\ \sigma_D^2$ in Eq. (5.3) is negligibly small and Eq. (5.8) was used for computing the RMS errors. The parameter σ_h was computed as the mean of the RMS elevation errors of the two end points of each line.

Table 14. Ground Coordinates of Pass Points in Panoramic Model 22/27

Point	X	Y	Z	RMS Errors X	RMS Errors Y	RMS Errors Z
	(meters)					
126	-36878.465	3120.151	339.285	7.373	5.600	16.933
118	-31540.133	3148.194	453.093	7.151	5.012	12.687
110	-26952.520	3297.808	348.501	7.274	5.341	15.215
103	-21628.828	3441.667	221.624	7.828	6.550	22.828
102	-21882.055	8968.773	184.357	7.790	6.508	22.471
109	-26421.641	9133.398	360.276	7.343	5.470	15.918
117	-31390.719	8952.133	387.427	7.162	5.028	12.732
125	-36802.652	8823.164	376.983	7.413	5.596	16.855
124	-37236.328	13243.367	326.652	8.044	6.132	18.420
108	-26955.492	13736.559	347.189	7.946	5.910	16.557
101	-22079.617	14134.652	340.022	8.456	6.967	23.155
107	-26595.426	19509.113	398.657	9.363	7.076	19.578
115	-31732.180	18990.473	605.118	9.175	6.668	17.015
123	-36733.367	18947.098	391.567	9.352	7.078	20.180
122	-36965.180	23179.227	1178.684	10.877	8.161	22.754
106	-27214.973	23757.707	397.051	10.642	8.041	21.600
127	-36165.941	-890.930	339.056	7.797	5.861	16.937
119	-31634.402	-1672.051	613.865	7.846	5.575	14.142
111	-24996.781	-1214.539	912.851	8.195	6.184	18.612
104	-21294.375	-1127.785	655.118	8.523	7.040	24.095
105	-21356.891	-6765.285	738.173	9.771	7.898	25.733
112	-25543.000	-6518.941	431.012	9.194	6.969	20.037
120	-31364.633	-4565.129	404.653	8.425	6.081	15.493
128	-36305.215	-5883.762	309.035	8.875	6.742	19.095

Table 15. RMS Errors in Slope

Point No. From	Point No. To	Horizontal Distance (D)	Elevation Difference (Δh)	Slope	σ_h*	RMS Error in Slope
		(meters)	(meters)		(meters)	
122	123	4,238	-787	-10° 31'	±21	±23'
123	117	11,333	- 5	- 0° 2'	16	± 7'
117	110	7,188	- 39	- 0° 19'	14	±10'
110	111	7,183	+565	+ 4° 30'	17	±11'
111	105	5,637	-175	- 1° 47'	22	±19'
115	117	10,044	-218	- 1° 15'	15	± 7'
117	118	5,806	+ 66	+ 0° 39'	13	±11'
118	119	4,821	+161	+ 1° 55'	13	±13'
119	120	2,906	-209	- 4° 07'	15	±25'

*σ_h was computed as the mean of the RMS elevation errors of the two end points.

6. CONCLUSIONS

Theoretically, the method of propagation of variance is a reliable means of evaluating the accuracy of an iterative least-squares solution only if the correction parameters converge to zero. However, simulation results in lunar phototriangulation showed that the method is also applicable to iterative least-squares solutions for which the following two conditions are achieved: 1) the corrections in the last iteration are smaller than the estimated standard errors of these parameters; and 2) the photogrammetric solution is well controlled to prevent any rapid accumulation of systematic errors.

Two computer programs have been successfully developed to use the method of propagation of variance to evaluate the relative and absolute accuracy of lunar phototriangulation. Programs SAPGO-A and THREED form an accuracy analysis package which may be used to perform the following functions in any phototriangulation project:

1) to predict the internal accuracy of photogrammetric solution (SAPGO-A);
2) to determine whether auxiliary data or ground controls of a specific accuracy can strengthen the solution (SAPGO-A);
3) to predict the accuracy of the final solution, including standard errors of both the triangulated pass points and the photo orientation parameters (SAPGO-A);
4) to determine the uncertainty in the tilt of the terrain surface defined by the computed pass points (THREED); and
5) to determine the absolute orientation accuracy of any stereomodel (THREED).

A simple expression was also developed for computing the standard error of the slope as a function of the standard error of the elevation at the two end points.

Simulation studies of the Apollo 15, 75-mm. photography showed that both the laser altimeter and the stellar camera measurements contributed significantly to improving the phototriangulation accuracy. A relative accuracy of ± 7 m. in the X and Y coordinates and ± 15 m. in the Z coordinates should be obtainable for the triangulated pass points

in a single stereo model even if the velocity vector has an RMS error of ±1.0 m./sec. At a tracking accuracy of ±0.1 m./sec. in the velocity vector, there was practically no degradation of accuracy due to error propagation in the phototriangulation process. At a tracking accuracy of ±0.5 m. and ±1.0 m. sec., the degradation in elevation accuracy is also negligible; but the accuracy in the X and Y coordinates degenerated at the rate of about 1 m. and 0.5 m. per model respectively.

Analysis of the AS-11-B1 measurements provided by NASA showed that the relative positional accuracy of the control points derived from one model of 76-mm. metric photography were: σ_X = ±15 m., σ_Y = ±10 m. and σ_Z = ±25 m. These RMS errors are approximately twice as large as those predicted from the simulation studies. This finding should not be surprising, because the simulation studies assumed a rather small RMS error of ±5 μm. for the image coordinates; whereas, the model coordinates actually measured from the AS-11-B1 were found to have an RMS error of ±10 μm. A lower image fidelity together with some unavoidable instrumental and human error in the AS-11-B1 measurements would then easily account for the larger RMS errors in the computed ground coordinates.

The control points derived from the 76-mm. photography could be used to orient the high-resolution models of panoramic photography with a relative accuracy of ±3 minutes of arc in the ω and κ rotations and ±7 minutes of arc in the ϕ rotation. Within the ±8.25° sweep area of the panoramic model, the relative position of any point in the model area could also be determined with an RMS error of ±15 m., ±10 m. and ±25 m. in the X, Y and Z coordinates respectively.

7. REFERENCES

1. Bevington, P. R., "Data Reduction and Error Analysis for the Physical Sciences," McGraw-Hill Book Co., New York, N.Y. 1969.
2. Brown, D. C., "A Matrix Treatment of the General Problem of Least-Squares Considering Correlated Observations," Ballistic Research Laboratory Report No. 960, Aberdeen Proving Ground, Maryland, October 1955.
3. Brown, D. C., "A Solution to the General Problem of Multiple Station Analytical Stereotriangulation", RCA Data Reduction Technical Report No. 43, February 10, 1958.
4. Brown, D. C., Davis, R. G., and Johnson, F. C., "Research in Mathematical Targeting -- The Practical and Rigorous Adjustment of Photogrammetric Net", Final Report, Contract No. AF 30(602)-3007. Prepared for Rome Air Development Center Griffiss Air Force Base, New York, October 1964.
5. Esenwein, G. F. et. al., "Apollo in Lunar Orbit", Astronautics and Aeronautics, Vol. 9, No. 4, April 1971, pp. 52-63.
6. Helmering, Raymond J.; Alspaugh, David; "Testing of the Apollo 15 Metric Camera System", Proceedings of the 1972 Fall Convention, American Society of Photogrammetry, October 11-14, 1972, pp. 65-111.
7. Lindgren, B. W., "Statistical Theory", The MacMillan Co., New York, 1965.
8. Madkour, M. F.; "Precision of Adjusted Variables by Least Squares", Journal of the Surveying and Mapping Division, Proceedings of the ASCE, 94:SU2, Sept. 1968, pp. 119-136.
9. Pope, A. J., "Some Pitfalls to be Avoided in the Iterative Adjustment of Nonlinear Problems", Proceedings of the 38th Annual Meeting, American Society of Photogrammetry, Washington, D. C., March 1972, pp. 449-477.
10. Wong, K. W.; and Elphingstone, G.; "Aerotriangulation by SAPGO", Photogrammetric Engineering, Vol. 38, No. 8, August 1972, pp. 779-90.
11. Wong, K. W.; "SAPGO-A Computer Program for the Simultaneous Adjustment of Photogrammetric and Geodetic Observations", Civil Engineering Studies, Photogrammetry Series No. 38, University of Illinois at Urbana-Champaign, Urbana, Illinois 61801.

12. Wong, K. W.; "THREED-A Computer Program for Three-Dimensional Transformation of Coordinates", Civil Engineering Studies, Photogrammetry Series No. 39, University of Illinois at Urbana-Champaign, Urbana, Illinois 61801.

CIVIL ENGINEERING STUDIES

PHOTOGRAMMETRY SERIES

The Photogrammetry Series publications are available through the National Technical Information Service, Operations Division, Springfield, Virginia 22151, USA, at $6.50 and up per paper copy and $1.45 per microfiche.

No.				N.T.I.S. Accession No.
1	1963	H. M. Karara	STUDIES IN SPATIAL AEROTRIANGULATION, Technical Report. No. 5, Engineering Experiment Station, University of Illinois.	
2	1965	A. A. Elassal	ANALYTICAL AERIAL TRIANGULATION THROUGH SIMULTANEOUS RELATIVE ORIENTATION OF MULTIPLE CAMERAS. (NSF-G-19749).*	PB 176 458
3	1965	Gordon Gracie	A STATISTICAL INVESTIGATION OF THE PROPAGATION OF RANDOM ERRORS IN ANALOG AEROTRIANGULATION. (NSF-G-19749).	PB 176 459
4	1966	M. F. Madkour	THE EFFECT OF THE ANOMALOUS GRAVITY ON THE DIRECTION OF THE VERTICAL AS DETERMINED BY A MECHANICALLY PERFECT INERTIAL PLATFORM. (NSF-GK-776).	PB 176 460
5	1967	H. F. Soehngen	STRIP AND BLOCK ADJUSTMENTS OF THE I.T.C. BLOCK OF SYNTHETIC AERIAL TRIANGULATION STRIPS. (NSF-GK-776).	PB 176 461
6	1967	D. C. O'Connor	VISUAL FACTORS AFFECTING THE PRECISION OF COORDINATE MEASUREMENT IN AEROTRIANGULATION.	AD 663 821
7	1967	D. E. Moellman	A COMPARATIVE STUDY OF TWO-PHOTO VERSUS THREE-PHOTO RELATIVE ORIENTATION. (NSF-GK-776).	PB 176 462
8	1967	H. F. Soehngen, C. C. Tung & J. W. Leonard	INVESTIGATION OF BLOCK ADJUSTMENTS OF I.T.C. FICTITIOUS BLOCK USING SECTIONS AND THE ITERATIVE AND DIRECT SOLUTIONS OF THE NORMAL EQUATION SYSTEM. (NSF-GK-776).	PB 179 567
9	1967	H. M. Karara	MONO VERSUS STEREO ANALYTICAL PHOTOGRAMMETRY -- Part I. (DA-1338-X).	AD 664 184

* Information in parentheses refers to the contract number of the project's sponsor.

CIVIL ENGINEERING STUDIES

PHOTOGRAMMETRY SERIES

(Continued)

No.				N.T.I.S. Accession No.
10	1968	G. Inghilleri	A TREATISE ON ANALYTICAL PHOTOGRAMMETRY (LECTURE NOTES).	PB 182 618
11	1967	S. Weissman	STEREOPHOTOGRAMMETRY AS A MEANS OF ANTHROPOMETRY FOR MENTALLY HANDICAPPED CHILDREN (MH-NB-07346-01A1).	PB 178 125
12	1968	D. E. Moellman & H. M. Karara	A UNIVERSAL DATA REDUCTION SCHEME FOR CLOSE-RANGE PHOTOGRAMMETRY (NSF-GK-1888).	PB 182 204
13	1968	S. Weissman	HORIZON-CONTROLLED ANALYTICAL AEROTRIANGULATION. (NSF-GK-776).	PB 178 030
14	1968	H. M. Karara & G. W. Marks	MONO VERSUS STEREO ANALYTICAL PHOTOGRAMMETRY -- Part II. (DA-1338-X).	AD 828 750
15	1968	H. M. Karara	ON THE PRECISION OF STEREOMETRIC SYSTEMS. (NSF-GK-1888).	PB 179 920
16	1968	K. W. Wong	GEOMETRIC CALIBRATION OF TELEVISION SYSTEMS FOR PHOTOGRAMMETRIC APPLICATIONS.	PB 182 715
17	1968	K. W. Wong	PHOTOGRAMMETRIC QUALITY OF TELEVISION PICTURES.	PB 182 727
18	1968	S. Weissman	ABOUT THE INCORPORATION OF HORIZON PHOTOGRAPHY IN ANALYTICAL AEROTRIANGULATION. (NSF-GK-776).	PB 180 783
19	1968	R. C. Malhotra	GRID PLATE CALIBRATION.	PB 182 728
20	1968	K. W. Wong	THREE COMPUTER PROGRAMS FOR STRIP AEROTRIANGULATION.	PB 186 469
21	1968	L. A. White	GRAPHICAL TRANSFORMATION AND COMPARISON OF PLANE COORDINATE SYSTEMS.	PB 182 716
22	1968	H. M. Karara & G. W. Marks	ANALYTICAL AERIAL TRIANGULATION FOR HIGHWAY LOCATION AND DESIGN (IHR-804).	PB 186 495
23	1969	J. M. Fry	METHODS OF GRAPHICAL AND ANALYTICAL MENSURATION OF SINGLE TERRESTRIAL PHOTOGRAPHS.	PB 183 889
24	1969	R. C. Malhotra	MATRIX TREATMENT OF THE ERROR ELLIPSOID (NSF-GK-1888).	PB 185 560
25	1969	K. W. Wong	GEOMETRIC FIDELITY OF THREE-SPACE TELEVISION SYSTEMS.	PB 187 466
26	1973	W. Faig	MODEL DEFORMATIONS DUE TO RADIAL LENS DISTORTION (NSF-GK-1888 and 11655).	
27	1971	J. J. Del Vecchio	LUNAR CONTROL BY ORBITAL TRIANGULATION-- AN ERROR ANALYSIS (RADC-TR-71-)	

CIVIL ENGINEERING STUDIES

PHOTOGRAMMETRY SERIES

(Continued)

No.				N.T.I.S. Accession No.
28	1971	R. C. Malhotra	HIGH-PRECISION STEREOMETRIC SYSTEMS (NSF-GK-1888).	
29	1972	G. W. Marks & H. M. Karara	IMAGE COORDINATE REFINEMENT ANALYSIS (RADC-F30602-20-C-0036)(RADC-TR-72-170).	AD 747 799
30	1971	K. W. Wong & G. Elphingstone	SIMULTANEOUS ADJUSTMENT OF PHOTOGRAMMETRIC AND GEODETIC OBSERVATIONS (SAPGO) (DA-ARO-D-31-124-G1129).	AD 737 748
31	1971	W. Faig	PHOTOGRAMMETRY AS A TOOL FOR HYDRAULIC SURFACE STUDIES. (University of Illinois Research Board).	PB 202 280
32	1971	W. Faig	DESIGN, CONSTRUCTION AND GEODETIC COORDINATION, OF A CLOSE-RANGE PHOTOGRAMMETRIC TEST FIELD. (NSF-GK-11655).	
33	1971	K. W. Wong, E. V. Gamble & R. E. Riggins	GEOMETRIC ANALYSIS OF THE RBV TELEVISION SYSTEM. (USGS 14-08-0001-12631).	PB 203 705
34	1971	K. W. Wong & N. G. Yacoumelos	TELEVISION DISPLAY OF TOPOGRAPHIC INFORMATION. (USATL-DAAK02-71-C-0045).	AD 734 367
35	1972	K. W. Wong	GEOMETRIC ANALYSIS OF THE RBV TELEVISION SYSTEM--PHASE II. (USGS 14-08-0001-12631).	
** 36	1973	Y. I. Abdel-Aziz & H. M. Karara	PHOTOGRAMMETRIC POTENTIALS OF NON-METRIC CAMERAS. (NSF-GK-11655).	
37	1974	K. W. Wong	TREATMENT OF CONTROL DATA IN LUNAR PHOTOTRIANGULATION (NAS9-12446).	
38	1974	K. W. Wong	SAPGOA- A COMPUTER PROGRAM FOR THE SIMULTANEOUS ADJUSTMENT OF PHOTOGRAMMETRIC AND GEODETIC OBSERVATIONS (DA-ARO-D-31-124-G1129).	
39	1974	K. W. Wong	THREED- A COMPUTER PROGRAM FOR THREE-DIMENSIONAL TRANSFORMATION OF COORDINATES (NAS9-12446).	

** In preparation.